Journal of Engineering Technology and Applied Sciences, 2022 *e-ISSN:* 2548-0391
Received 9 June 2021, Accepted 30 October 2021 *Vol. 7, No. 1, 1-30*
Published online 21 March 2022, Research Article *doi: 10.30931/jetas.950046*

Citation: Busby, M., Green, D., Combrinck, M., "A Computational Fluid Dynamic Investigation of a Data Centre Employing Rear Door Heat Exchangers". Journal of Engineering Technology and Applied Sciences 7 (1) 2022 : 1-30.

A COMPUTATIONAL FLUID DYNAMIC INVESTIGATION OF A DATA CENTRE EMPLOYING REAR DOOR HEAT EXCHANGERS

Michael Busby[a*], David Green[b], Madeleine Combrinck[a]

[a]Department of Mechanical and Construction Engineering, Northumbria University, England
*mbusby722@hotmail.com (*corresponding author), madeleine.combrinck@northumbria.ac.uk*

[b]Capital Projects Group, Estate Management, University of Cambridge, England
david.green@admin.cam.ac.uk

Abstract

As the global demand for data services expands, cooling in data centres continues to evolve towards more efficient and cost-effective systems. Incorporating active rear door heat exchangers has become a popular and reliable method that increases the capability of data centres to operate at higher power densities. This study conducts a thermal analysis of a data centre employing active rear door heat exchangers with the use of computational fluid dynamic (CFD) techniques. The data centre under investigation contains seventy-seven cooled racks with three additional uncooled racks operating in the centre of the hall. The main purpose of this study is to understand how the uncooled racks affect the temperature distribution in the data centre. This study presents a modelling technique which uses temperature and velocity field measurements to facilitate the modelling of rear door heat exchangers. Computer server modelling server was carried out at varying inlet temperature and load. Server simulation results have been utilized with field measurements to create four data centre scenarios. Scenarios were created to show how inlet temperature and load affect the temperature distribution in the data centre. Data centre scenarios have been used to validate and compare with field measurements performed. It was found that heat dissipation in the server was directly related to the server's velocity profile. From the data centre scenarios created it was found that when higher loaded racks are isolated amongst lower loaded racks the distribution of heat is less significant than if the higher loaded racks were situated in clusters of three or more. It was also found that higher loaded racks could be positioned strategically to diminish the effect of the untreated air produced by the uncooled racks in the data centre. The findings from this paper help to understand the thermal behaviour in data centres and suggests areas to consider when reviewing pre-existing data centre designs.

Keywords: Data centre, server, thermal management, CPU, heatsink, convection, rear door heat exchanger

1. Introduction

Data centres form the backbone upon which a wide variety of IT services are built. They can be defined as computer warehouses that store large amounts of data for different organisations to meet their daily transaction processing needs [1]. Data centres provide a network of storage and computing resources which deliver shared software applications and data. Applications range from email and file sharing to Big Data, communications, and collaboration services. Data centres are essential to the successful operation of digital enterprises and are designed to support business applications such as data storage, management, back-up, and recovery services. They are also utilised in research and development applications for advanced computing facilities with powerful research computing tools, cluster computing and on-site computing laboratories [2]. Complying with service-level agreement requirements is paramount for IT organisations and as a result data centres are required to operate 24/7, 365-days a year with low level maintenance plans [3]. Most of the world's Internet Protocol (IP) traffic is computed via data centres, according to the International Energy Agency global IP traffic increased almost threefold during 2014-18 and project similar growth for 2018-22 [4]. A rapid increase in cloud computing, high performance computing and the vast growth in internet use has ignited the importance of energy consumption in data centres [5]. Computer Processing Unit (CPU) power density has increased rapidly since 1990. The power generated from CPUs is dissipated in the form of heat, heat removal in data centres is one of the most essential yet least understood of all critical IT environment processes [6]. A hybrid-cooled system employing a rear door heat exchanger combines the benefits of both air and liquid cooled systems. Hybrid cooled systems can save energy and increase reliability with straightforward installation as well as providing an effective cooling solution for high density data centres. A global interest for high levels of connectivity and Big Data, is putting strain on data centres to operate effectively. The increase in demand means data centres are operating at much higher power density than before. This rapid rise in growth has increased the need for improved thermal management in data centres.

A study by Chi, YQ et al [7], conducted an energy and performance comparison between two cooling solutions adopted in data centres. The paper modelled a High-Performance Computing (HPC) configuration at the University of Leeds using an air-water hybrid cooled system and compares with a hypothetical model of an immersed liquid-cooled system. The study utilized a management software to monitor server component temperatures and calculated the heat flux generated from the temperature differential across the server. The study provides a favourable insight into the thermal performance of HPC systems, however there is limited investigation into the thermal management of a hybrid cooled system at room level.

A study by J. Cho et al [8], considered six types of air distribution system commonly used in data centres. The study constructed a Computational Fluid Dynamics (CFD) model to analyse the air distribution for six cases employing Computer Room Air Conditioning (CRAC) units for cooling. The study presents a strong analysis of air distribution and thermal management in data centres with power density between 3-5kW/rack. Air-cooled systems in data centres are limited to lower rack power density and become more redundant as power density increases.

A study conducted by Almoli, A et al [9], investigated the performance of rear door heat exchangers. This CFD study modelled airflow through a server with a porous medium to simulate the effect of small geometric features present in a server. Six racks with three different heat loads were investigated to determine how a hybrid cooled system (passive/active) acts in conjunction with CRAC units. Modelling the airflow inside a server more accurately would

provide a greater understanding of the thermodynamic conditions and develop a more robust modelling technique for data centres.

A study by Choi, J et al [10], presents a CFD-based modelling tool called ThermoStat for studying temperatures in data centres. The tool presented is validated with the use of field measurements taken at different locations at a rack and server level. The nature of the tool utilizes CFD techniques to provide a complete 3D profile of the temperature within the system. An excellent methodology is presented for simulating thermal distribution at a rack level; however, the study fails to investigate the thermal management of a data centre at a room level.

Inadequate cooling in data centres can lead to inefficiencies such as air recirculation causing hot spots. Hot spots put strain on cooling infrastructure to operate efficiently and can have a significant impact on thermal management in data centres [11]. Hot spots can arise in both air-cooled and hybrid-cooled systems due to the heat transfer medium being air in both cases. Hybrid-cooled systems are less likely to generate hot spots because they employ localised heat exchangers at each rack. Air-cooled systems contain heat exchangers in the form of CRAC units which are usually positioned at the end of each isle. The hot air produced from the back of the racks is drawn through CRAC units to be cooled and then recirculated into the room. Air-cooled systems require a greater distance for hot air to travel and therefore poor design can lead to inefficiencies and hot spots. This study models a data centre which primarily employs rear door heat exchangers. The data centre also includes three populated racks which do not contain localised heat exchangers that have been installed post completion. Racks which do not contain localised heat exchangers have no additional cooling infrastructure in place and are free to exhaust hot air into the room. Due to a steady ambient room temperature of 25-26°C these racks can maintain safe operating conditions which fall within recommended ASHRAE guidelines. This study aims to analyse the thermal behaviour originating as a result of racks with no additional cooling. The study also looks at how load, inlet temperature and uncooled rack configurations can affect the temperature distribution in the data centre.

2. Materials and methods

2.1 Server model description

A Dell Poweredge 1750 rack-mounted server was modelled as the server geometry as shown in Fig 1. The specification of the Poweredge 1750 is displayed in Table 1. The components which have been modelled in the server are displayed in Table 2. Heat sources in the server have been modelled with constant surface temperature. To understand a range of server loading scenarios and to validate with experimental data collected, inlet temperatures were modelled every 2°C, ranging from 24-28°C. Heatsink and temperatures assigned for each loading condition are shown in Table 3, corresponding server fan and inlet velocity are shown in Table 4.

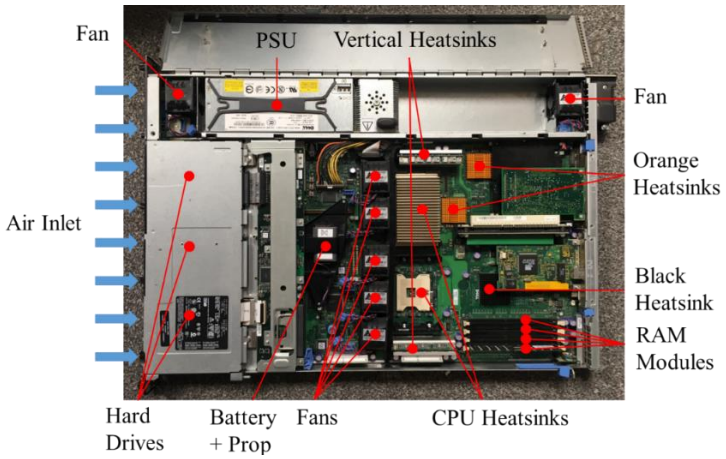

Figure 1. Dell Poweredge 1750 rack-mounted server

Table 1. Server – Specification

Dell Poweredge 1750 Specification	
Dimensions	44.7cm x 68.3cm x 4.2cm
Power	320W
Voltage	100-240 VAC, 50/60 Hz, 3,9-2.0 A
Heat Dissipation	1026 BTU/hr (max/power supply)

Table 2. Server – Components

Component	**Quantity**	**Volume/unit (cm^3)**
Fan	7	68.45
CPU Heatsink	2	80.50
Black Heatsink	1	12.15
Orange Heatsink	2	4.79
Vertical Heatsink	2	15.84
Power Supply Unit (PSU)	1	320.14
RAM Module	4	11.97
SCSI Hard Drive	3	311.39
Battery + prop	1	46.54

Table 3. Server – Loading conditions

Load	**CPU Heatsinks (°C)**	**Other Heatsinks (°C)**	**PSU (°C)**
Idle	Inlet T + 1°C	Inlet T + 1°C	Inlet T + 1°C
Medium	40	30	35
High	60	35	45
V.High	75	40	55

Table 4. Server – Air velocity conditions

Load	**Inlet Velocity (m/s)**	**Fan Velocity (m/s)**
Idle	0.25	7.81
Medium	0.50	13.50
High	1.50	19.20
V.High	2.30	21.50

2.2 Rack model description

Each rack was split into five sections to replicate five cooling fans at the back of a rack. Sections 1 and 5 contained nine racks and 2, 3 and 4 contained eight, equalling a 42U rack enclosure. The server loading conditions; idle, medium, high, and very high, were used to create low, medium, and high rack loading scenarios, as shown in Fig 2. The physical geometry of the chilled water network and fans at the back of the rack were not modelled using CFD techniques. The back of rack temperature was modelled using middle of the rack and cooled back of the rack temperatures collected from the ColdLogik user interface. The ColdLogik user interface provided a single set of data for each rack. The temperature difference between the middle of the rack and cooled back of the rack was plotted with the temperature at the middle of the rack, as shown in experimental results section, 3.1, Graph 1. The reference point created in the server (plane 3) was used to replicate the middle of the rack temperature provided by the ColdLogik user interface. The temperature results obtained at plane 3 were used to calculate an average middle of the rack temperature for each section of the rack. The temperatures generated for each section of a rack were then used to calculate one average middle of the rack temperature per rack. The line of best fit generated in Graph 1, was used to predict the temperature difference between the average middle of the rack temperature and the temperature which would be produced at the back of the rack. The temperature difference was subtracted from the middle of the rack temperature to calculate the cooled back of the rack temperature. The back of rack temperature was calculated for low, medium, and high rack loading conditions with varying inlet temperature. To model the effect of different inlet temperatures at the front of the rack, the rack was split into symmetrical top/bottom sections. It has been assumed that the temperature exhausted at the back of the rack is constant across all 5 fans. A similar method was used to identify the back of rack fan velocity for each rack loading condition, based on several field measurements taken in the hall.

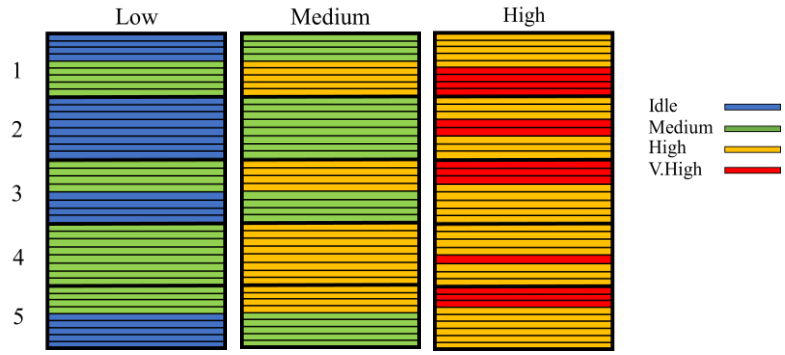

Figure 2. Rack – Loading arrangement

2.3 Data hall model description

Low, medium, and high rack loading conditions were used to create 4 separate data hall scenarios, B-E. From modelling a range of inlet temperatures at server level, data hall scenarios were created with varying inlet temperature and load. Scenario C was created to replicate the condition of the data hall at the time of field measurement collection. Therefore, scenario C was used for direct comparison and validation of the model with the experimental data collected. Scenarios B, D and E were created to study the effects of varying inlet temperature and load in the hall. The data hall contains 77 cooled racks, 12 spare cooled racks and 3 uncooled racks in the centre of the hall with the option of an additional uncooled rack. Rack loading conditions were split into low, medium, and high operating states, operating specification for each scenario is shown in Table 5.

Table 5. Data hall - Loading scenarios

Scenario	Load					Inlet Temperature Range (°C)
	Cooled Racks (77)			Uncooled Racks (4)	Spare Cooled Racks (12)	
B	L (23)	M (0)	H (54)	No Load	No Load	24 - 28
C	L (29)	M (16)	H (32)	M (3)	No Load	24 - 28
D	L (10)	M (11)	H (56)	M (4)	No Load	24 - 28
E	L (0)	M (0)	H (77)	M (4)	H (12)	24 - 28

2.4 Experimental Methods

The 10.8m x 13.2m x 3m data hall under investigation employs rear door heat exchangers with five fans at the back of each rack. Each rack contains its own array of chilled water pipes at the rear, with fans 250mm in diameter. Temperature readings were taken at various locations inside the data hall, monitoring locations recorded are displayed in Fig 3 and 4. Figs 3 and 4 show the data hall arrangement from a bird's eye view. The five locations shown in Fig 3, were monitored at a height of 1.8m for four consecutive days. The locations shown in Fig 4, were monitored at a height of 620mm and 1240mm, centred and at the front of the racks, for a minimum of five hours per location. Locations 13, 15 and 19 in Fig 4, were positioned at the exhaust side of uncooled racks located in the centre of the data hall. Temperature data was also collected from a rack monitoring interface provided by the installer, ColdLogik. The ColdLogik temperature readings were located at three single points across each rack shown in Fig 5. The ColdLogik user interface provided a temperature at the front of the rack, the middle of the rack and the rear of the rack once the air has been cooled. Racks labelled 'BS1' and 'BH1' for example, denote the first spare and uncooled racks in row B.

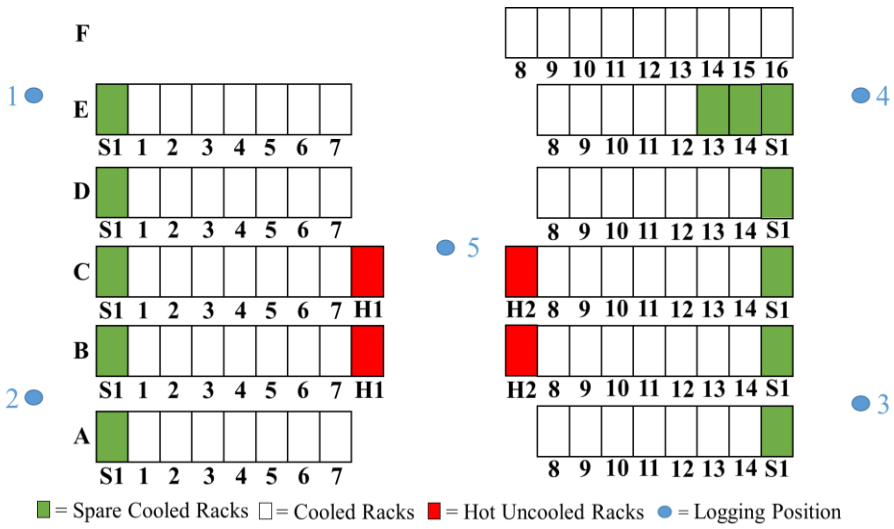

Figure 3. Data hall - Room monitoring

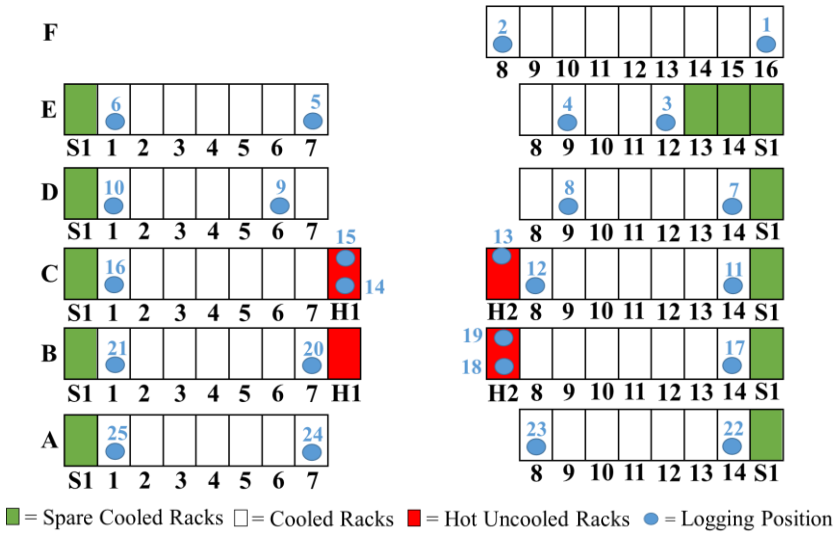

Figure 4. Data hall – Row monitoring

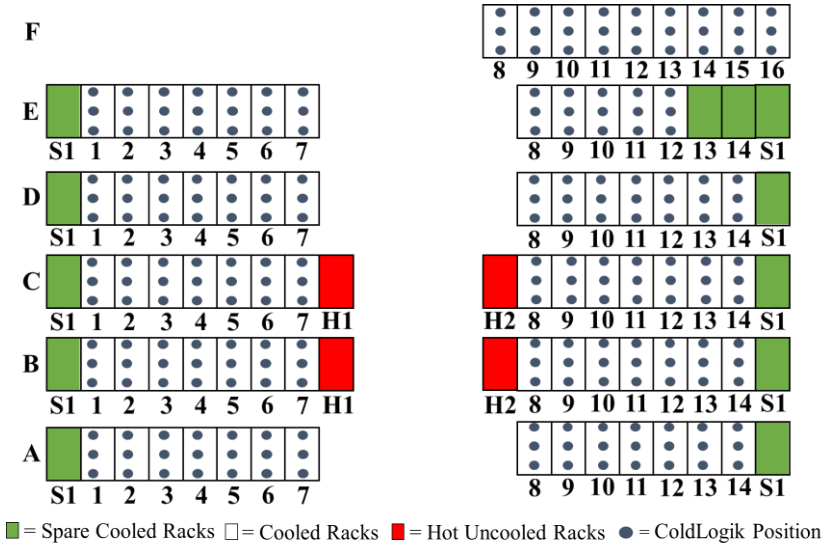

Figure 5. Data hall - Installer monitoring (ColdLogik)

2.5 Numerical methods

The governing equations for fluid dynamics are the conservation laws for mass, momentum, and energy. For Newtonian fluids the governing equations can be expressed as follows [12]:

Continuity Equation; $$\frac{\partial \rho}{\partial t} + \frac{\partial (\rho u_i)}{\partial x_i} = 0$$

Momentum Equations; $$\frac{\partial (\rho u_i)}{\partial t} + \frac{\partial (\rho u_j u_i)}{\partial x_j} = S_i - \frac{\partial p}{\partial x_i} + \mu \frac{\partial^2 u_i}{\partial x_j \partial x_j}$$

Energy Equations; $$\frac{\partial (\rho e)}{\partial t} + \frac{\partial (\rho u_j e)}{\partial x_j} = -p \frac{\partial u_i}{\partial x_i} + \Phi + \frac{\partial}{\partial x_i}\left(\mathrm{K} \frac{\partial T}{\partial x_i}\right)$$

The governing equations for momentum are known as the Navier-Stokes equations. The time averaged properties are of greatest interest in turbulent flow fields. The governing equations for steady mean flow are known as the Reynolds-Averaged Navier-Stokes (RANS) equations. These are obtained by introducing Reynolds decomposition, which decomposes the flow variables into steady and fluctuating components.

RANS Equations; $$\frac{\partial(\rho\bar{u}_i)}{\partial t} + \frac{\partial(\rho\bar{u}_j\bar{u}_i)}{\partial x_j} = \bar{S}_i - \frac{\partial\bar{p}}{\partial x_i} + \mu\frac{\partial^2\bar{u}_i}{\partial x_j\partial x_j} - \frac{\partial\left(\rho\overline{u_i'u_j'}\right)}{\partial x_j}$$

The RANS equations are obtained by using the Reynolds decomposition in the Navier-Stokes equations and taking the time average [12]. The depiction of turbulence can have profound effects on the usefulness of a numerical solution in CFD. Turbulence modelling justification is essential for robust CFD modelling [13].

2.6 Selecting a turbulence model

The flow field inside the server is assumed to contain a mixture of turbulent and laminar flow regions due to the high fan speeds when operating at high loads.

A study conducted by Choi, J et al, presented a CFD based modelling tool for studying temperature in rack mounted servers. Choi, J et al, aimed to understand and modulate the processor temperature in a server as a function of its load. The study utilized the LVEL model, which is an algebraic turbulence model specifically developed for low Reynolds number flow regimes [10]. The two-equation k-ω Shear Stress Transport (SST) model uses a blending function to gradually transition from near the wall, where it uses the standard k-ω model, to a high Reynolds number version of the k-ε model in the outer portion of the boundary layer. This allows the k-ω SST model to transition better between laminar and turbulent flow regions. A study by Milnes, J et al [14], on assessment of RANS models for Hypervapotron flow and heat transfer, showed that when the k-ω SST model was applied to a sufficiently fine grid, it gave the most accurate predictions of heat transfer and single-phase cavity flow.

A study by Wibron, E et al [12], examined the performance of different turbulent models, for CFD modelling of data centres at a room level. The turbulence models studied were the most commonly used k-ε model, the Reynolds Stress Model (RSM) and Detached Eddy Simulations (DES). It was found that the k-ε model failed to predict the low velocity regions at heights above the rack, the paper indicates that RSM should be used to model turbulent flow in data centres. The RSM can occur high computational costs due to a high-quality mesh requirement [15].

A turbulence optimization study was carried out to determine the appropriate turbulence model for the server simulations. A laminar flow model and four turbulence models were tested as shown in Table 6. Turbulence models tested included the k-ε, k-ε RNG, k-ω SST and the RSM models.

A reference point in the server was taken at plane 3, as shown in Fig 6, to compare the outcome of the study. The study concluded that the k-ω SST model was the most adequate and was therefore used for the CFD modelling of the server and data hall. Plane 3 generated the highest average temperature in the server and was used to validate server simulations with the experimental data collected.

Table 6. Server – Turbulence modelling comparison

Model	Convergence Time	Average Temperature Plane 3 (T_m) (°C)
Laminar	25 min	34.28
k-ε	45 min	37.40
k-ε RNG	1 hr 10 min	37.25
k-ω SST	1 hr	38.89
RSM	1 hr 30 min	37.49

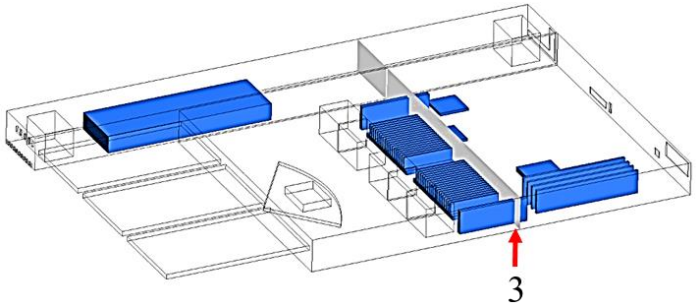

Figure 6. Server Model reference point (plane 3)

2.7 Model parameters

Table 7. Server & Data Hall – CFD Model settings

Server Model	
Dimensions	44.7cm x 68.3cm 4.2cm
Grid Cells	1,980,000
Turbulence Model	k-ω SST
Gravitational Force	Off
Energy Equation	On
Convergence Time	1 hr

Table 8. Server – CFD simulation parameters

Data Hall Model	
Dimensions	10.8m x 13.2m x 3m
Grid Cells	11,270,000
Turbulence Model	k-ω SST
Gravitational Force	Off
Energy Equation	On
Convergence Time	2 hr

Table 9. Data hall - CFD simulation parameters

Fluent Settings	
Solver	Pressure Based (Steady)
Scheme	SIMPLE
Gradient	Least Squares Cell Based
Pressure	Second Order
Pressure-Velocity Coupling	Coupled
Density	Second Order Upwind

Momentum	Second Order Upwind
Turbulent Kinetic Energy	Second Order Upwind
Specific Dissipation Rate	Second Order Upwind
Energy	Second Order Upwind
Residual Monitors	
Continuity	$1x10^{-4}$
x-velocity	$1x10^{-4}$
y-velocity	$1x10^{-4}$
z-velocity	$1x10^{-4}$
Energy	$1x10^{-6}$
k	$1x10^{-4}$
ω	$1x10^{-4}$
Reference Values – Fluid	
Fluid	Air
Density (kg/m^3)	Ideal Gas Law
Specific Heat (C_p) (J/kgK)	1006.43
Thermal Conductivity (W/mK)	0.0242
Viscosity (kg/ms)	Sutherland
Molecular Weight (kg/kmol)	28.966
Reference Values – Solid	
Solid	Aluminium
Density (kg/m^3)	2719
Specific Heat (C_p) (J/kgK)	871
Thermal Conductivity (W/mK)	202.4

3. Results

3.1 Experimental results

As mentioned previously the cooling architecture of the rear door heat exchangers was not modelled using CFD techniques. Instead, the experimental data was used to determine the cooling effect of the rear door heat exchangers. The reference point created in the server model was used to compare the middle of the rack temperatures generated from server modelling with the middle of the rack temperatures collected experimentally. Graph 1 shows the derived relationship between experimental middle of rack and cooled back of rack temperatures.

3.2 Numerical Results

3.2.1 Server Model Validation

The average temperature at plane 3 has been used to validate the middle of the rack temperature provided experimentally by the ColdLogik user interface data. The data provided by the ColdLogik user interface consisted of one middle of the rack temperature per rack. This data is provided by ColdLogik so that the data centre operators can daily monitor the temperature at each rack. The ColdLogik data collected contains inlet temperature ranging from 25.1-28.1°C. The simulated results show idle to very high loading condition with inlet temperature ranging from 24-28°C.

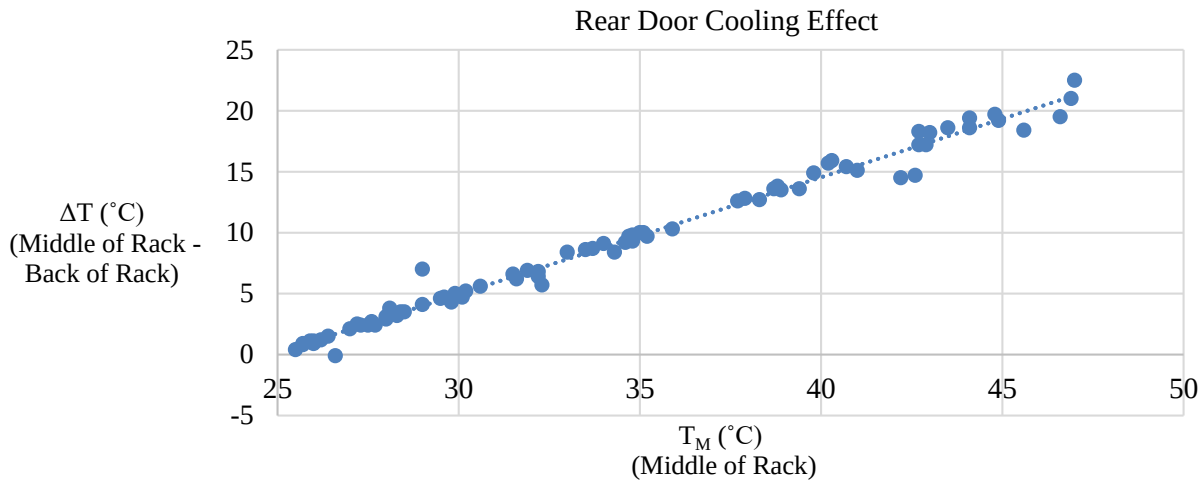

Graph 1. Rear Door Heat Exchangers – Cooling effect

To validate the simulated results with the experimental data, an inlet temperature of 26°C has been selected as shown in Graph 3. It can be seen from Graph 2; most of the experimental data lies within the idle and very high loading results. The four loading conditions selected for server modelling produced temperatures at plane 3 which were in good correlation with the experimental data provided by ColdLogik. Even though there are many possible server loading conditions, the four loading conditions selected for server modelling fall within the middle of the rack temperature range provided from the experimental data. Validation of the server simulations with experimental data allows for more robust modelling of the data hall.

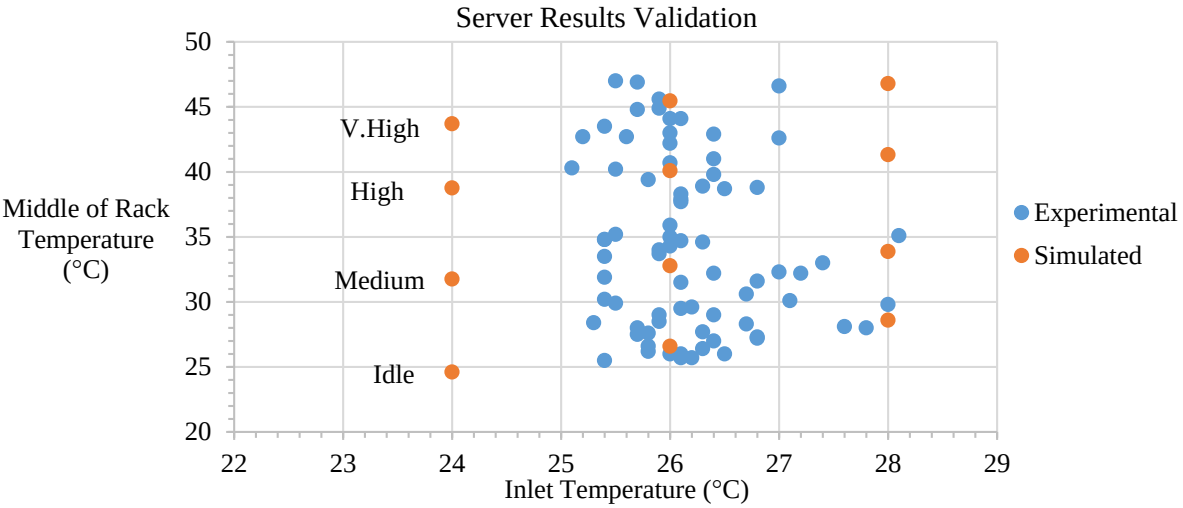

Graph 2. Server Results – Validation

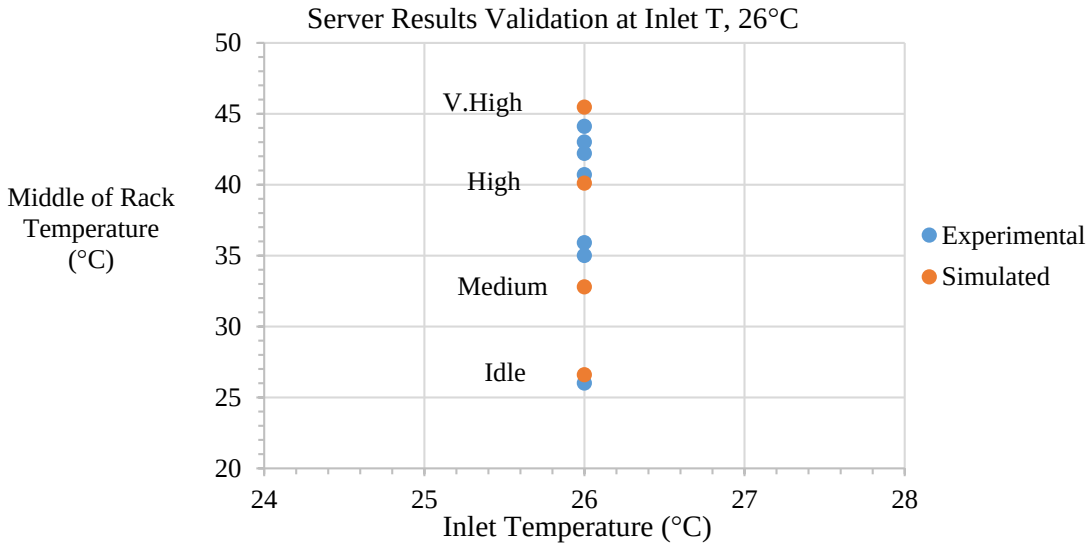

Graph 3. Server Results – Validation at inlet T, 26°C

3.2.2 Data hall model validation

The data hall under investigation contains three uncooled racks in the centre of the hall. Scenario C represents the data hall in its current state with the experimental inlet temperature and loads applied to this scenario. Scenario C was used to validate the experimental data collected. Other scenarios created contain 'what if?' scenarios to analyse the effect of inlet temperature, load, and uncooled rack configurations. To compare the experimental data collected, the logging locations used were recreated for each data hall scenario. Graph 5 shows the temperature comparison at monitoring locations 1-5 for scenario C. As expected, the uncooled racks in the centre of the hall generated a higher temperature at location 5, shown in Fig 3. The average error margin for scenario C was found to be 1.83 percent. For scenario B the average error margin was 3.00 percent. The error across monitoring locations 1-5 in scenario B is evenly distributed except for location 5. Scenario B does not contain operated uncooled racks in the centre of the hall, because of this the deviation at location 5 was 7.59 percent. The lowest average error margin of 1.43 percent occurred for scenario E. This is unexpected as scenario E contained a significant increase in heavily loaded racks compared to scenario C. When analysing the cooling effect of the rear door heat exchangers, the calculated back of rack temperature, T_B, ranged from 24.98-25.68°C for all server simulation results. Due to this the cooled racks modelled in all scenarios show a close resemblance to the experimental data collected. This implies that modelling of the uncooled racks has the greatest thermal influence in the model. Scenario E contained an extra uncooled rack in the centre of the hall compared to scenario C. This additional uncooled rack reduced the error margin at location 5 from 2.11 percent to 0.45 percent. This suggests that the uncooled racks could be modelled more accurately to the current uncooled racks operating in the data hall.

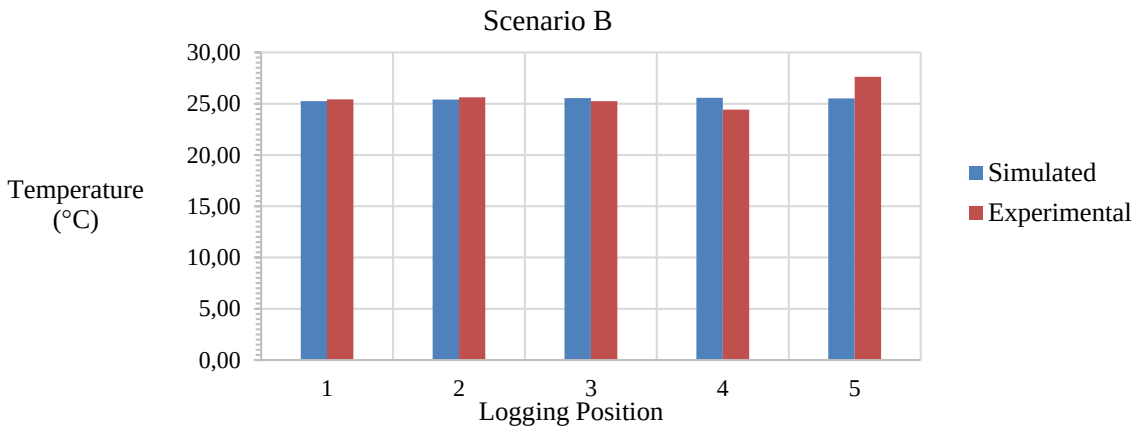

Graph 4. Scenario B – Results comparison (room monitoring)

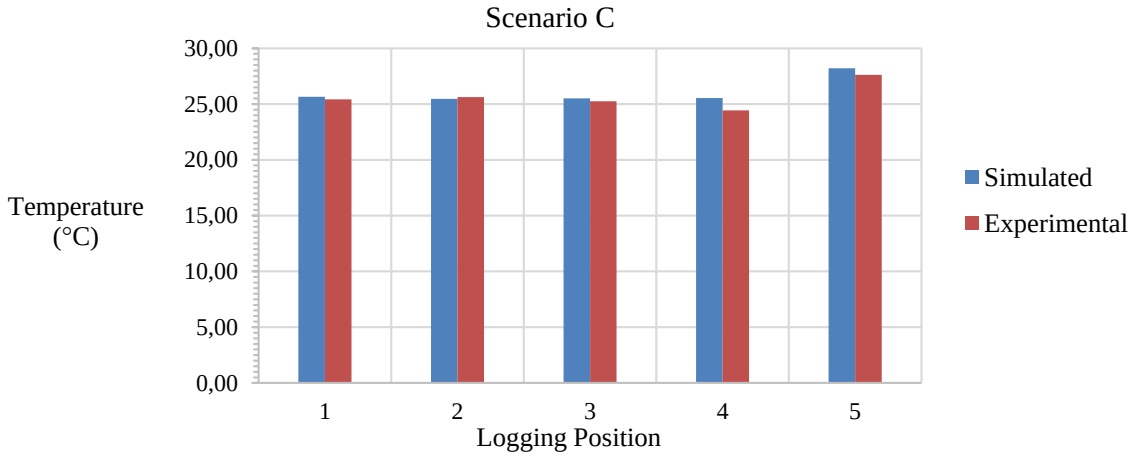

Graph 5. Scenario C – Results comparison (room monitoring)

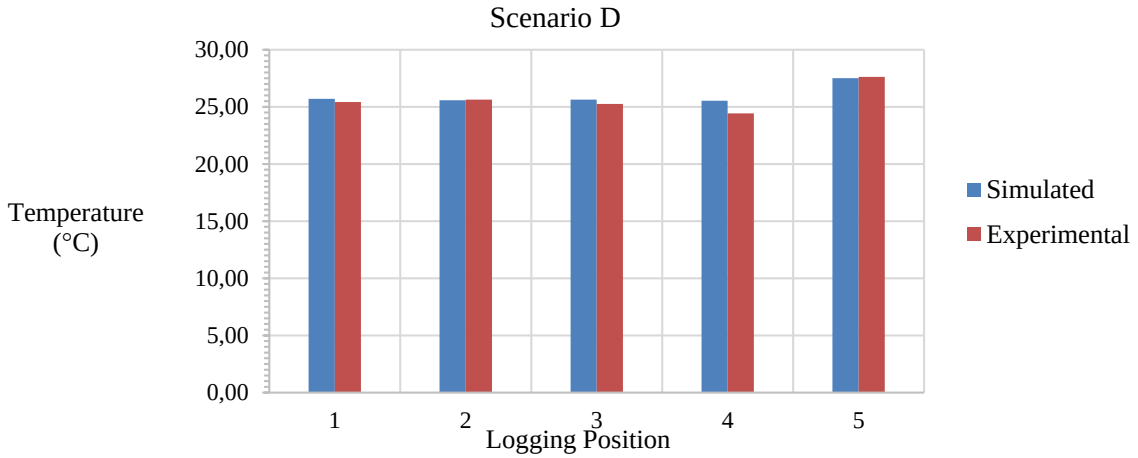

Graph 6. Scenario D – Results comparison (room monitoring)

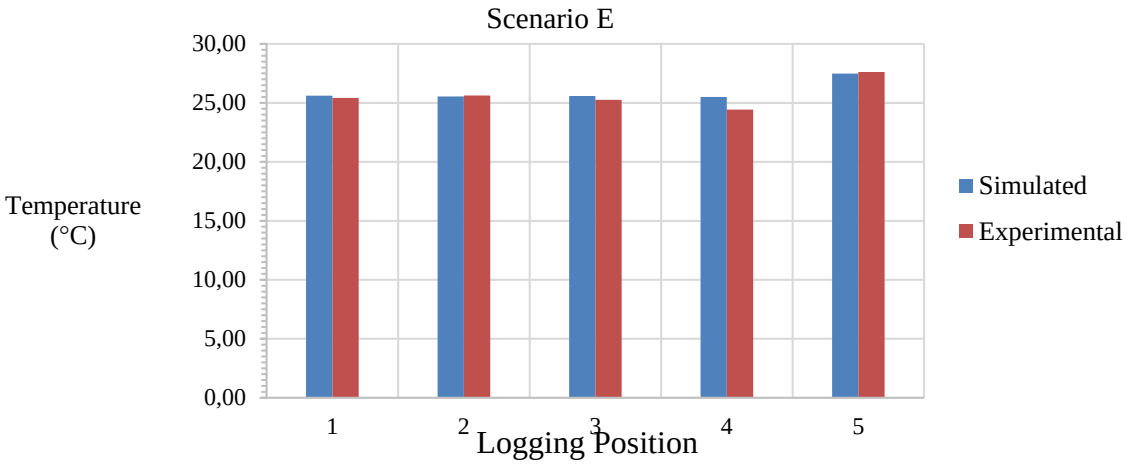

Graph 7. Scenario E – Results comparison (room monitoring)

Row monitoring locations 1-25 used for comparison are shown previously in Fig 4. Locations 13, 15 and 19, recorded the back of rack temperature of uncooled racks in the centre of the hall. Temperature of top and bottom sections were recorded at each location. To compare the uncooled back of rack temperatures for experimental and simulated results, the back of rack temperature values for each scenario have been plotted on separate graphs. Three graphs have been plotted for each scenario showing the comparison between back of rack temperatures at 13, 15 and 19, and front of rack temperatures at 1-25 (excluding 13, 15 and 19). Graphs 8-19 show the comparison at these locations for scenario B-E.

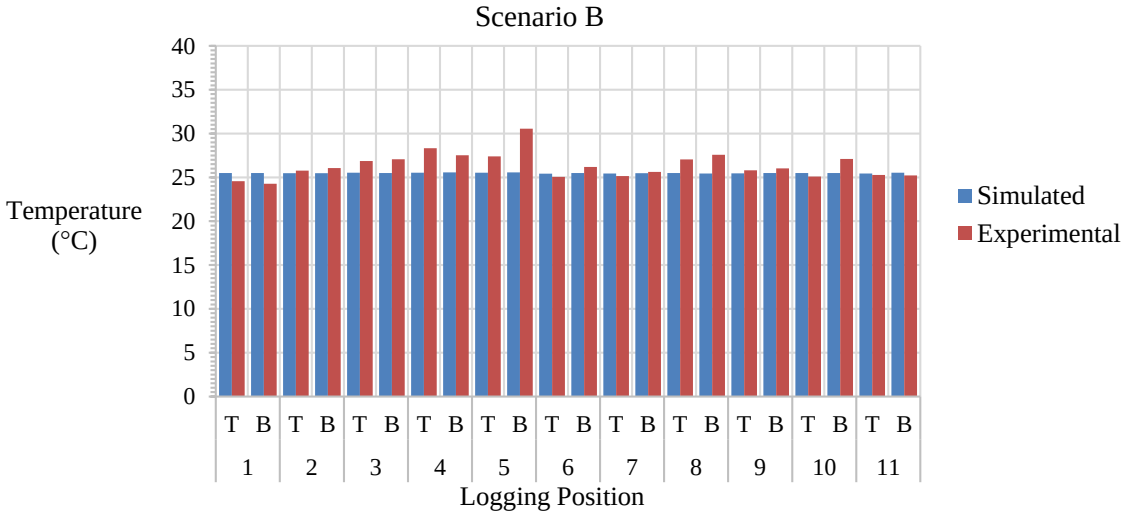

Graph 8. Scenario B – Results comparison (row monitoring)

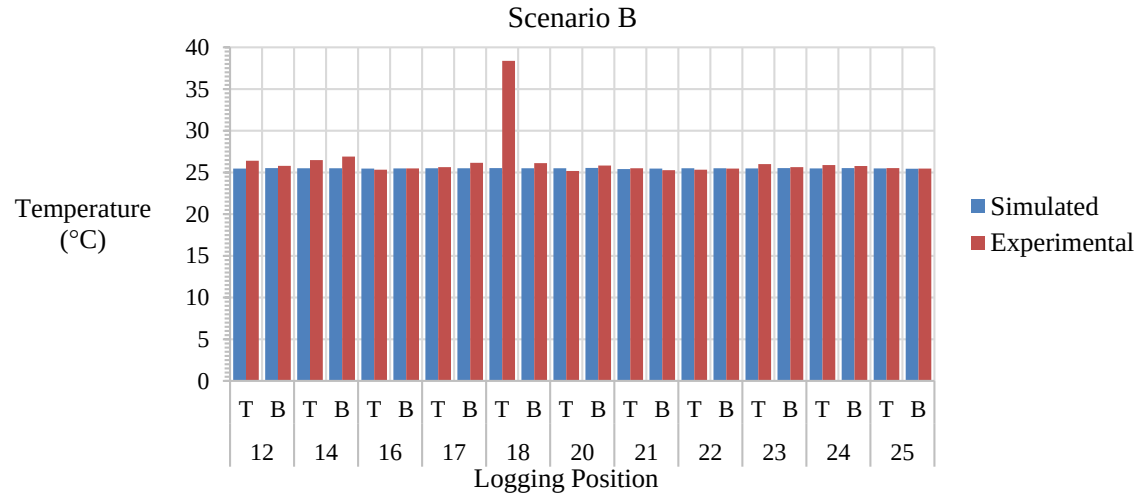

Graph 9. Scenario B – Results comparison (row monitoring)

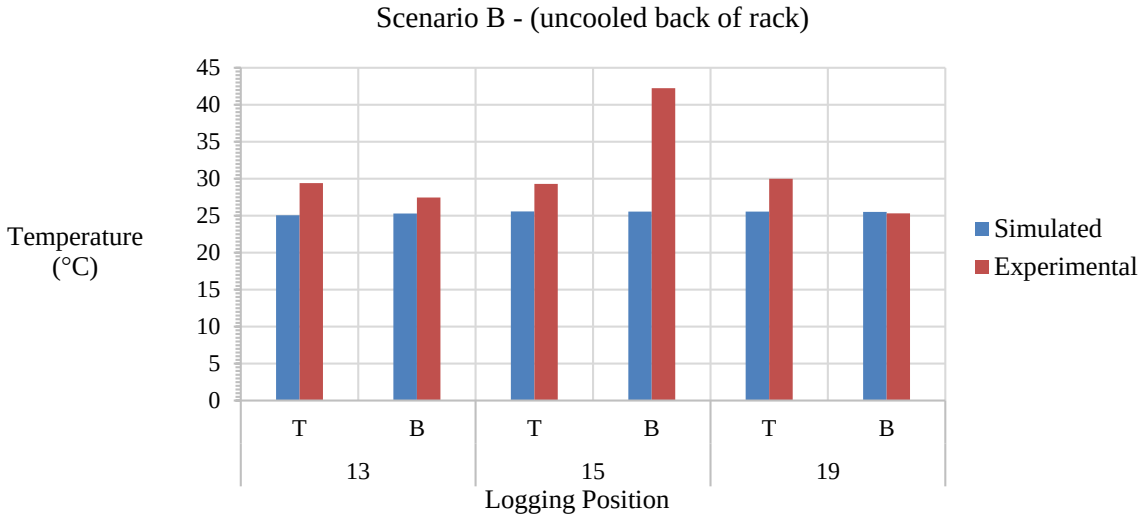

Graph 10. Scenario B – Results comparison (row monitoring)

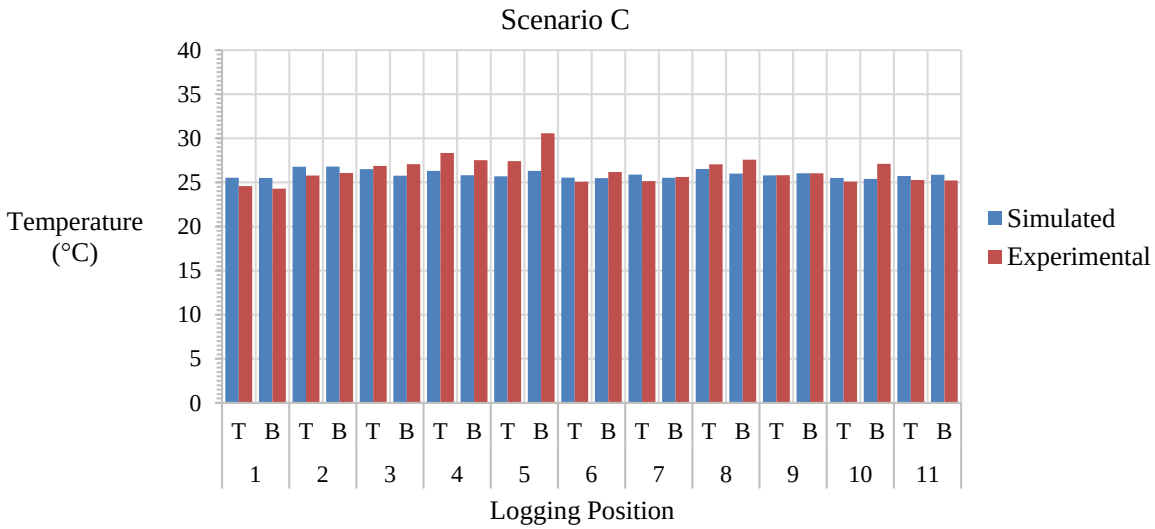

Graph 11. Scenario C – Results comparison (row monitoring)

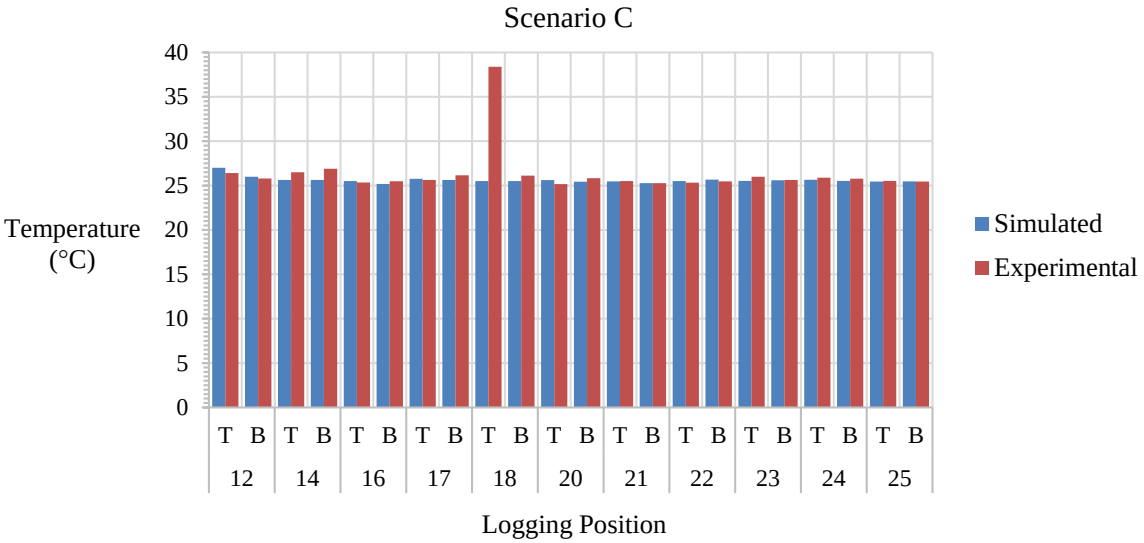

Graph 12. Scenario C – Results comparison (row monitoring)

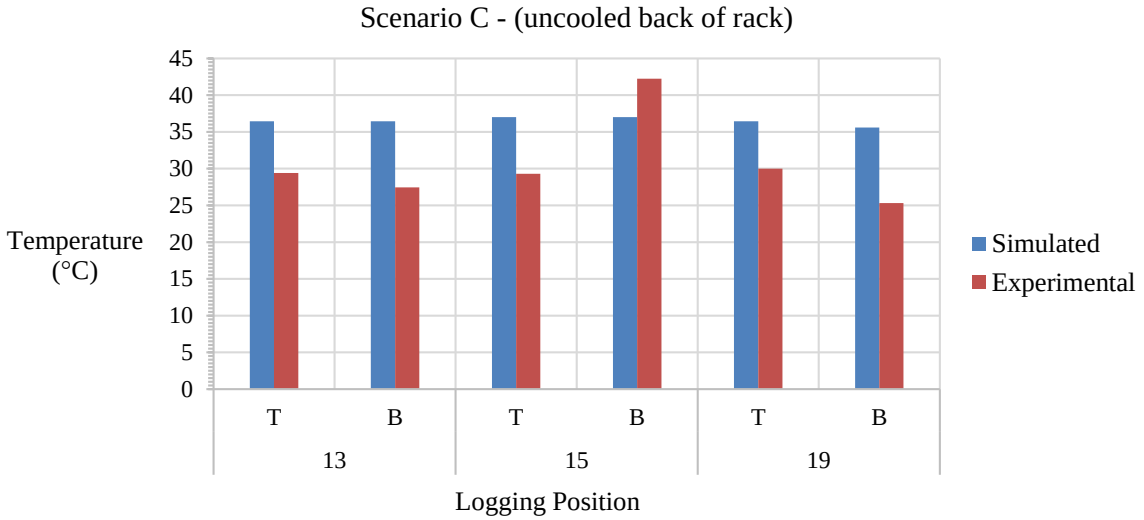

Graph 13. Scenario C – Results comparison (row monitoring)

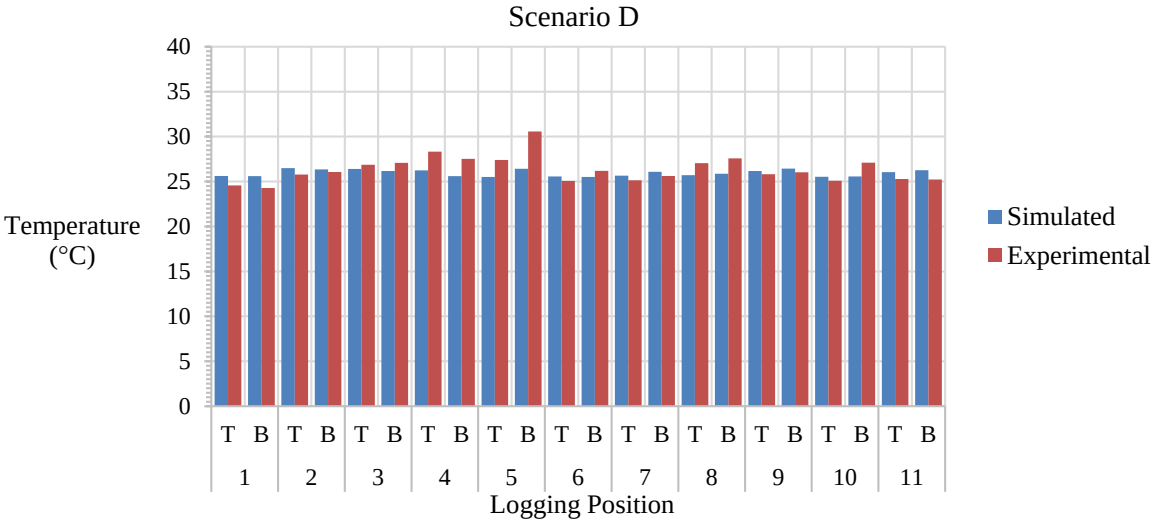

Graph 14. Scenario D – Results comparison (row monitoring)

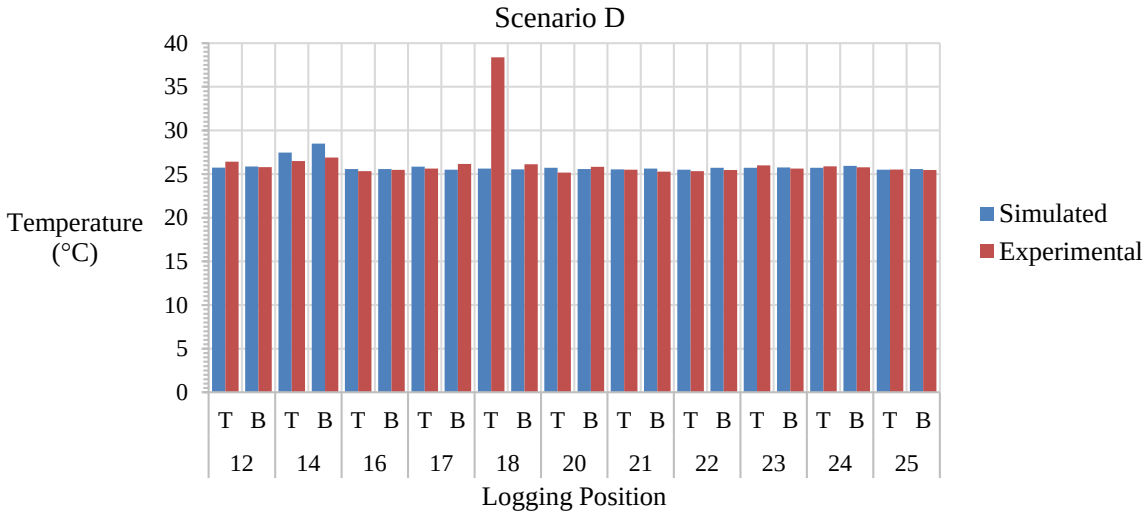

Graph 15. Scenario D – Results comparison (row monitoring)

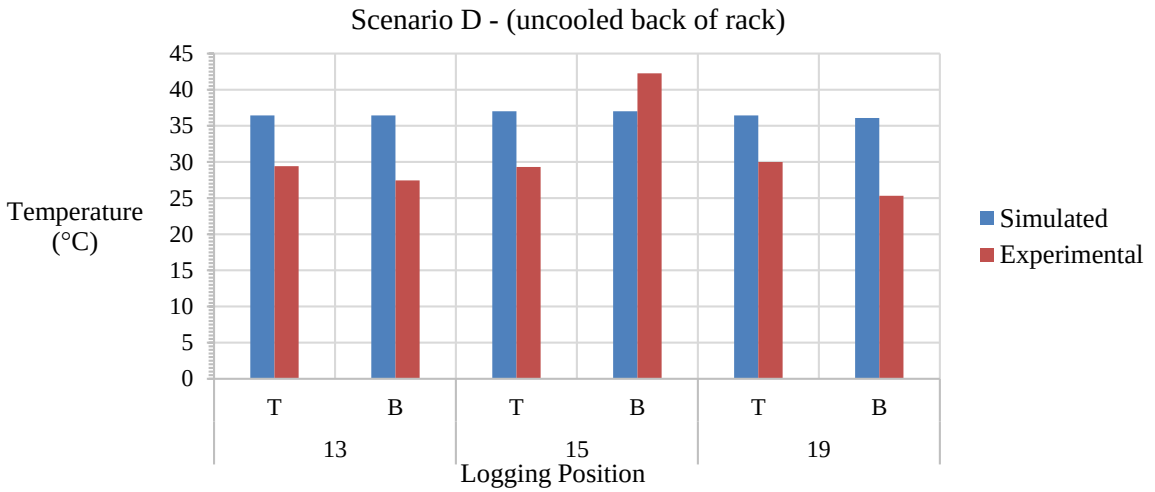

Graph 16. Scenario D – Results comparison (row monitoring)

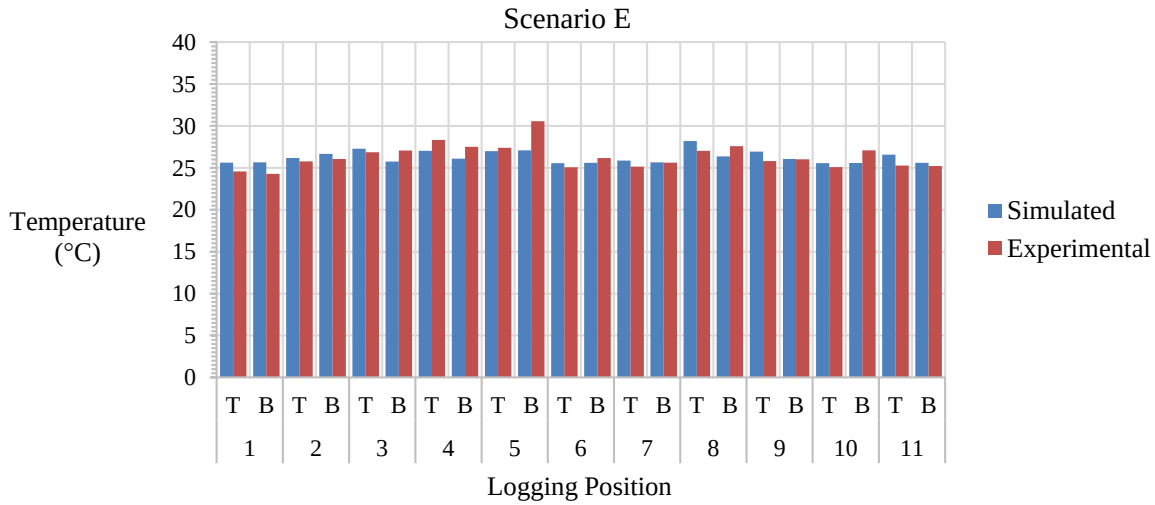

Graph 17. Scenario D – Results comparison (row monitoring)

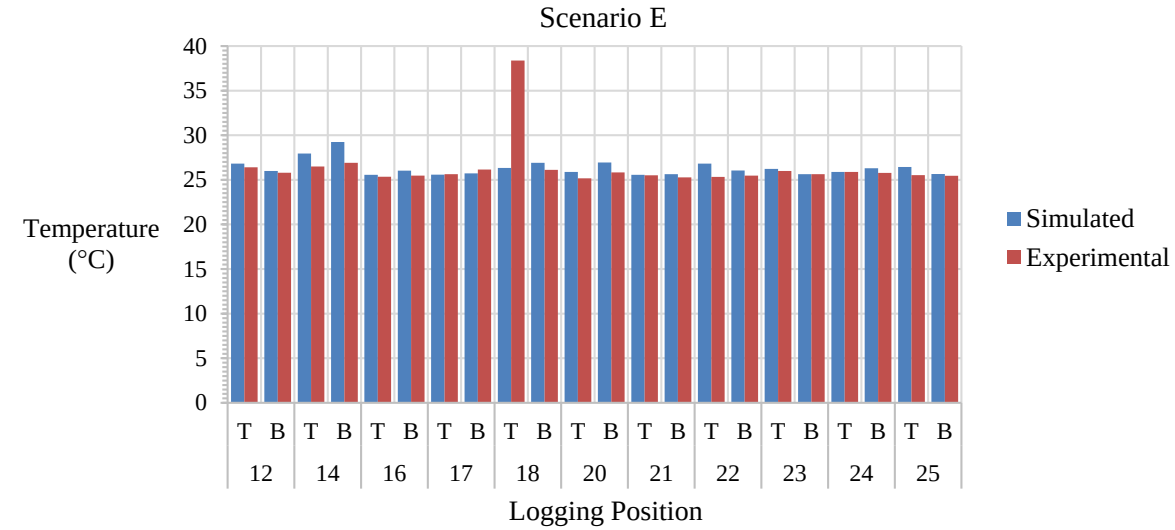

Graph 18. Scenario E – Results comparison (row monitoring)

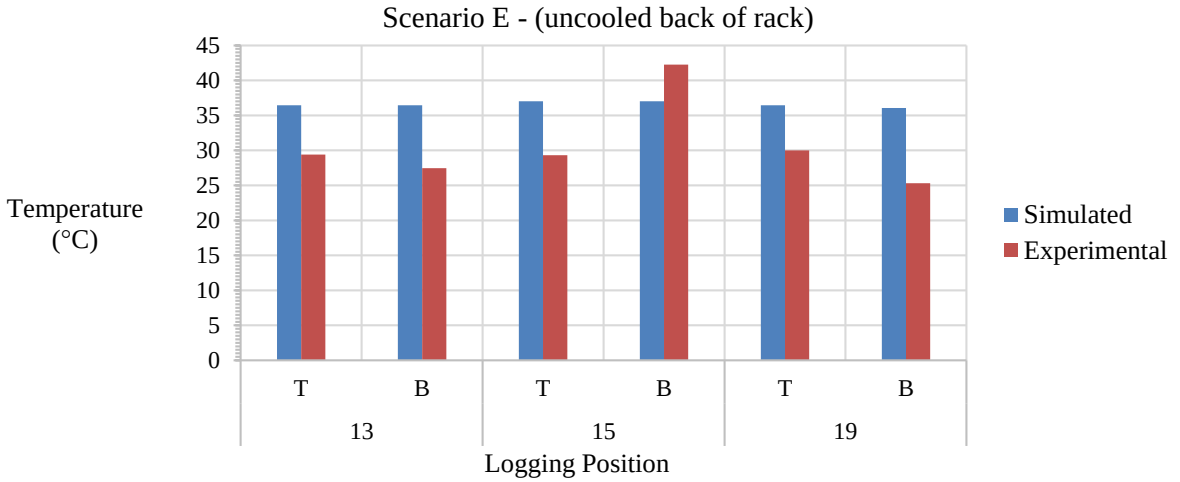

Graph 19. Scenario E – Results comparison (row monitoring)

Row monitoring comparison for scenario C can be seen in Graphs 11-13. Graphs 11 and 12 show an evenly distributed error except for a few locations such as 3, 4, 5 and 18. The average error margin for cooled locations excluding 3, 4, 5 and 18 was 1.88 percent. The average error margin at locations 3, 4, and 5 was 6.30 percent. The error produced at the top half of the rack at location 18 was 33.53 percent. At the time of experimental data collection, the uncooled rack at location 18 was populated with ten servers at the top half the rack and an empty bottom half of the rack. The elevated temperature recorded at the top half of location 18 is expected to have occurred due to hot air being recirculated from the back of the rack.

From Graph 13, the measured temperature at the bottom of location 15 is around 5°C more than the simulated results at that location. It is expected that the higher temperature originating from location 15 has resulted in the higher front of rack temperatures measured at locations 3, 4 and 5.

The average error margin from modelling the uncooled racks for scenario B, C, D and E were 15.08, 26.24, 26.56 and 26.54 percent respectively. Scenario B produced the lowest error between results however, scenario B largely underestimates the temperature at these locations due to the absence of uncooled racks in the model. The simulated results at uncooled rack locations 13, 15 and 19 for scenario C, D and E, generate a temperature around 36°C. The

measured temperature at these locations ranges from 25.32-42.25°C. This suggests that the uncooled racks measured operate at levels higher than levels modelled in scenario C-E. The uncooled racks in this project were modelled at full capacity to analyse the effect of employing heavily populated uncooled racks. In reality the uncooled racks contained several empty spaces which did not occupy servers. The variation in temperature at measured uncooled locations is a result of occupied and empty server slots in the racks.

3.2.3 Server model

The reference point generated in the server (plane 3), generated the highest average temperature in the model. Temperature and velocity distribution at plane 3 has been interpreted with the help of contours. The temperature and velocity distribution at plane 3 is presented in Fig 7-30, to compare server conditions at varying inlet temperature.

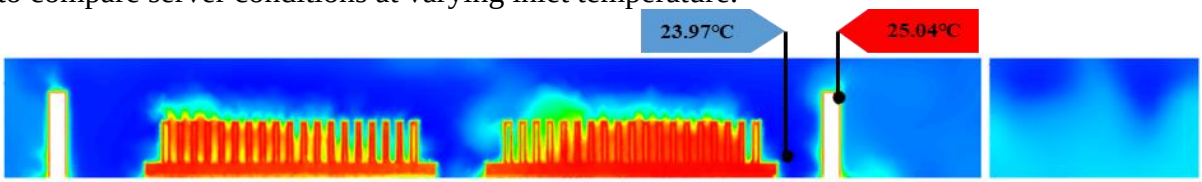

Figure 7. Temperature distribution (Inlet T = 24°C, Load = Idle)

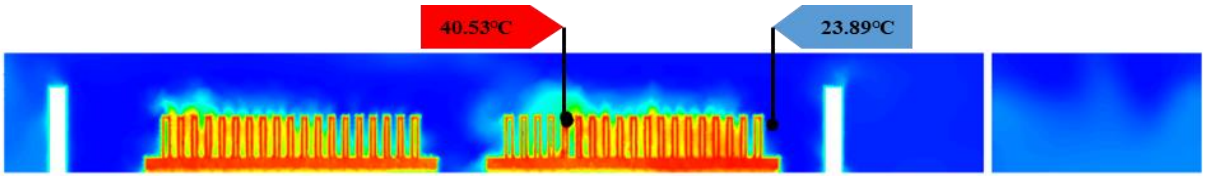

Figure 8. Temperature distribution (Inlet T = 24°C, Load = Medium)

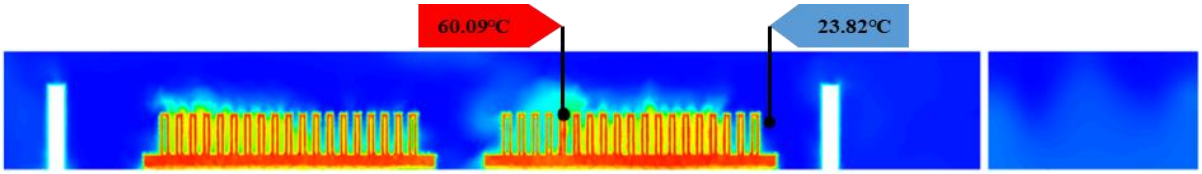

Figure 9. Temperature distribution (Inlet T = 24°C, Load = High)

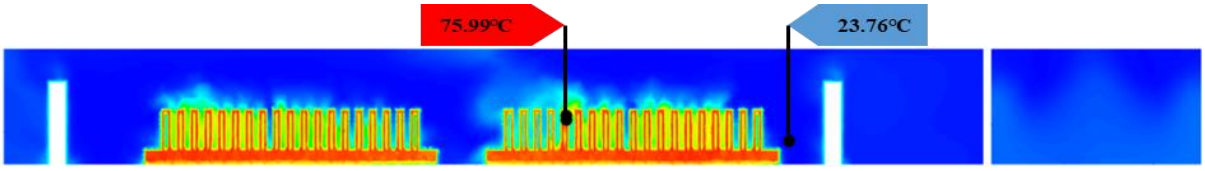

Figure 10. Temperature distribution (Inlet T = 24°C, Load = High)

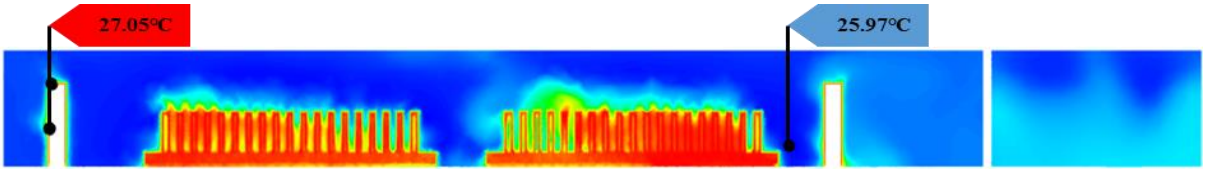

Figure 11. Temperature distribution (Inlet T = 26°C, Load = Idle)

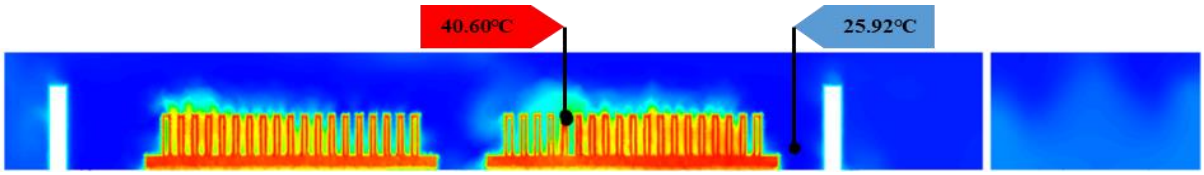

Figure 12. Temperature distribution (Inlet T = 26°C, Load = Medium)

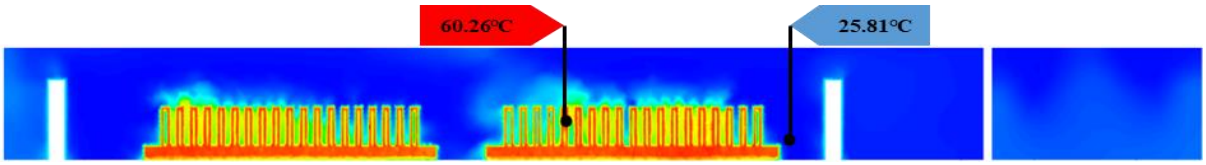

Figure 13. Temperature distribution (Inlet T = 26°C, Load = High)

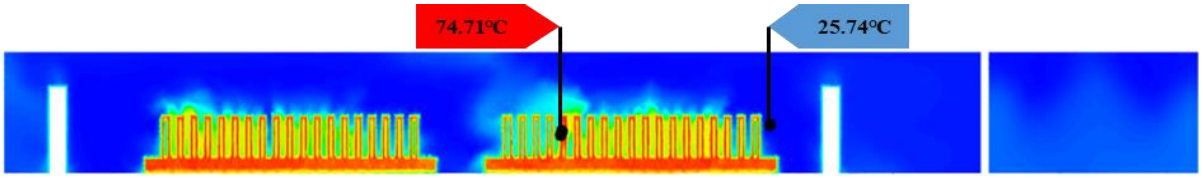

Figure 14. Temperature distribution (Inlet T = 26°C, Load = V. High)

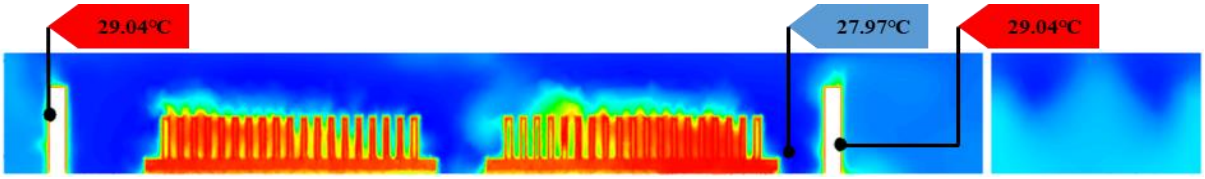

Figure 15. Temperature distribution (Inlet T = 28°C, Load = Idle)

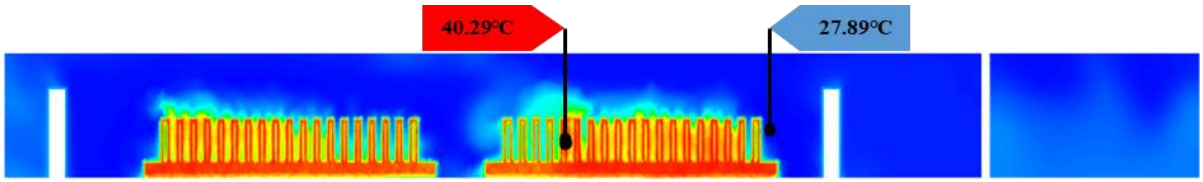

Figure 16. Temperature distribution (Inlet T = 28°C, Load = Medium)

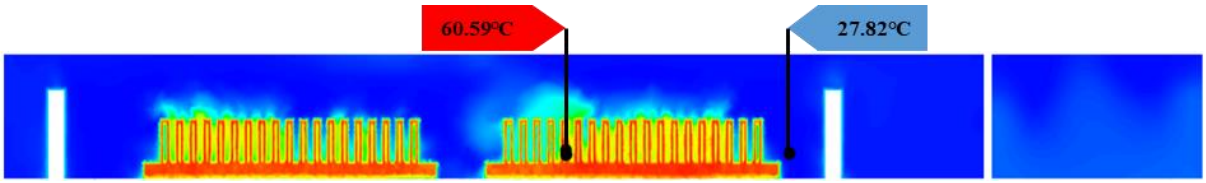

Figure 17. Temperature distribution (Inlet T = 28°C, Load = High)

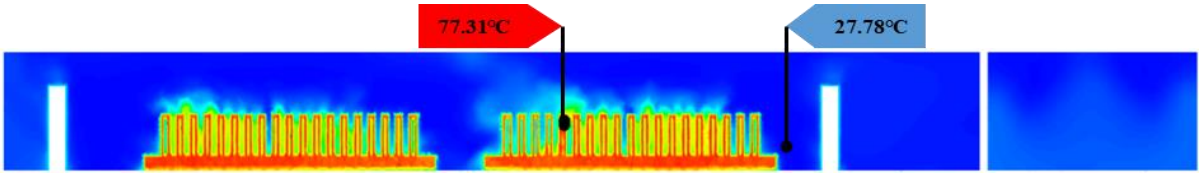

Figure 18. Temperature distribution (Inlet T = 28°C, Load = V. High)

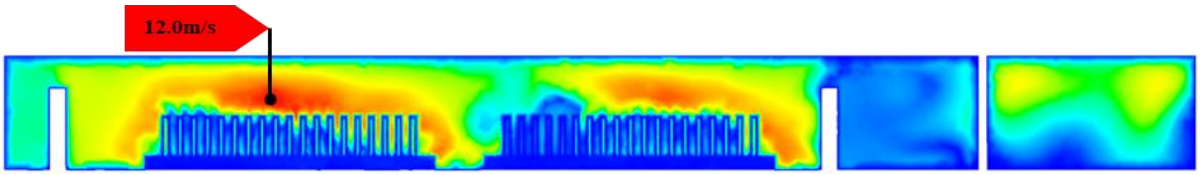

Figure 19. Velocity distribution (Inlet T = 24°C, Load = Idle)

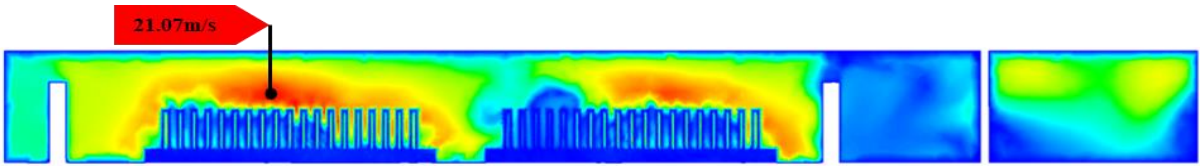

Figure 20. Velocity distribution (Inlet T = 24°C, Load = Medium)

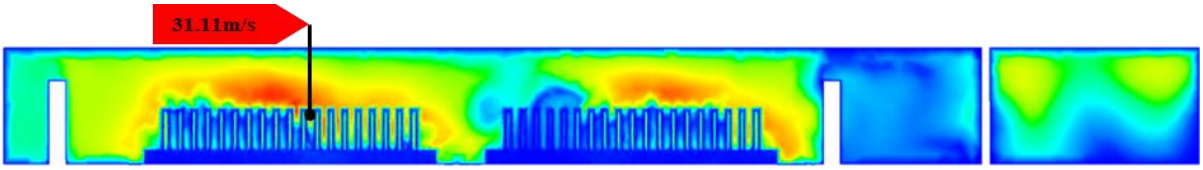

Figure 21. Velocity distribution (Inlet T = 24°C, Load = High)

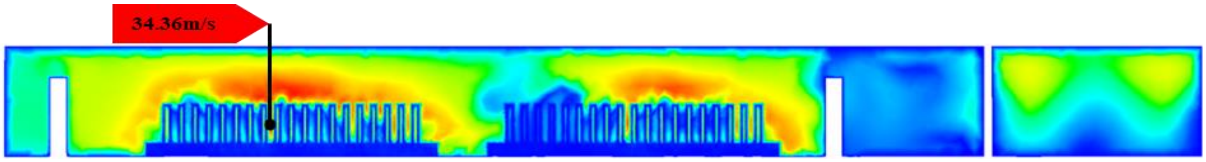

Figure 22. Velocity distribution (Inlet T = 24°C, Load = V. High)

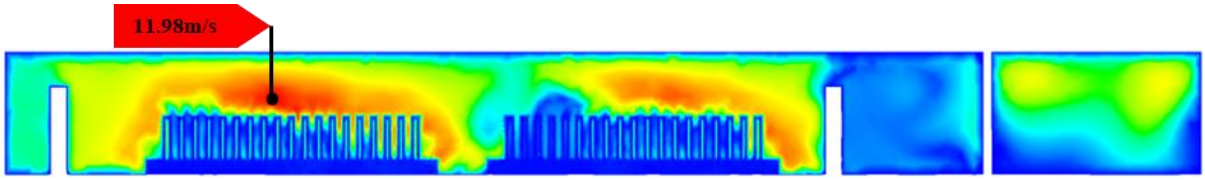

Figure 23. Velocity distribution (Inlet T = 26°C, Load = Idle)

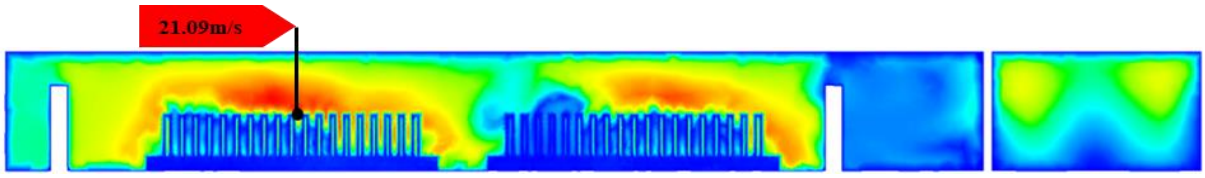

Figure 24. Velocity distribution (Inlet T = 26°C, Load = Medium)

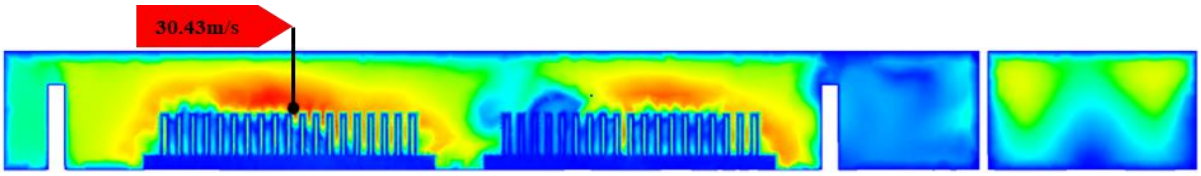

Figure 25. Velocity distribution (Inlet T = 26°C, Load = High)

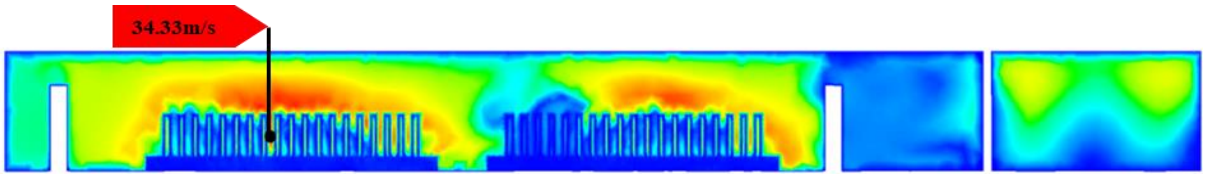

Figure 26. Velocity distribution (Inlet T = 26°C, Load = V. High)

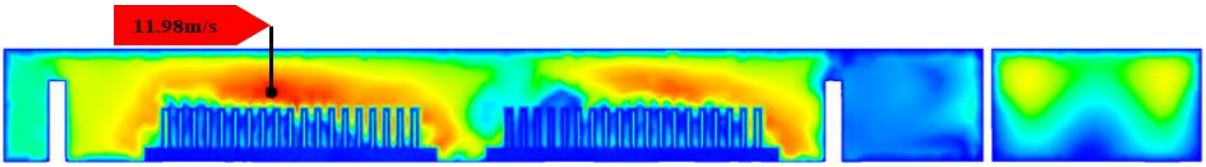

Figure 27. Velocity distribution (Inlet T = 28°C, Load = Idle)

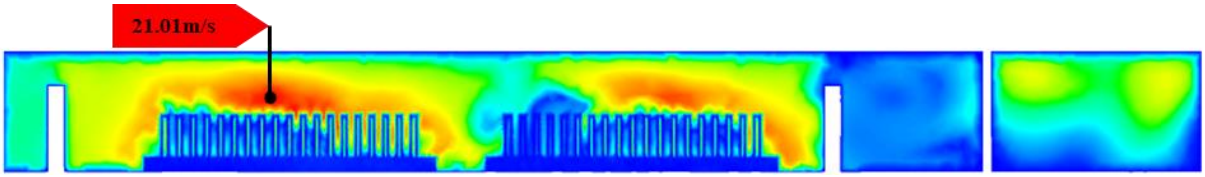

Figure 28. Velocity distribution (Inlet T = 28°C, Load = Medium)

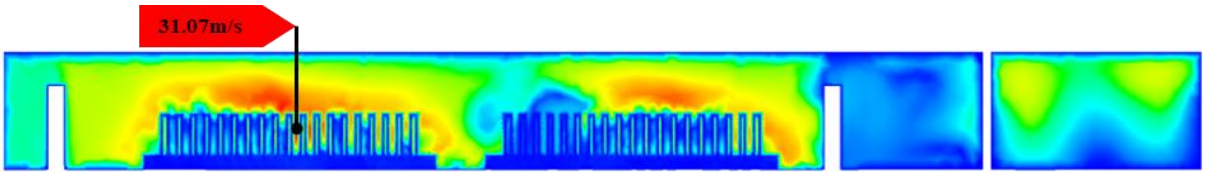

Figure 29. Velocity distribution (Inlet T = 28°C, Load = High)

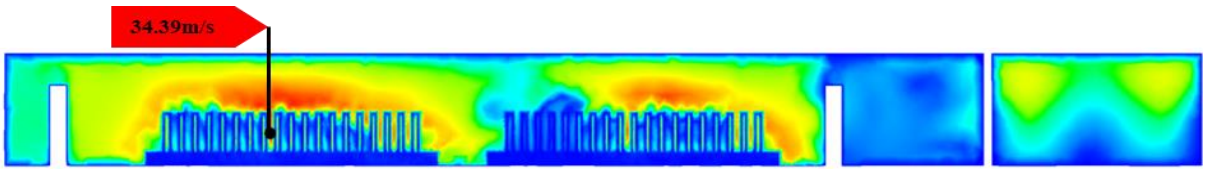

Figure 30. Velocity distribution (Inlet T = 28°C, Load = V. High)

3.2.4 Data hall model

To analyse the temperature distribution for each data hall scenario, Figs 31, 35, 39 and 43 were created to show highly loaded racks and inlet temperatures. 'High inlet temperature' refers to the highest inlet temperature areas which are relevant to that scenario. Figs 32, 36, 40 and 44 show the resulting temperature distribution at the front of the racks for each scenario. Temperature and velocity distribution at 1m on the XY plane has been presented to study the resulting distribution for each scenario.

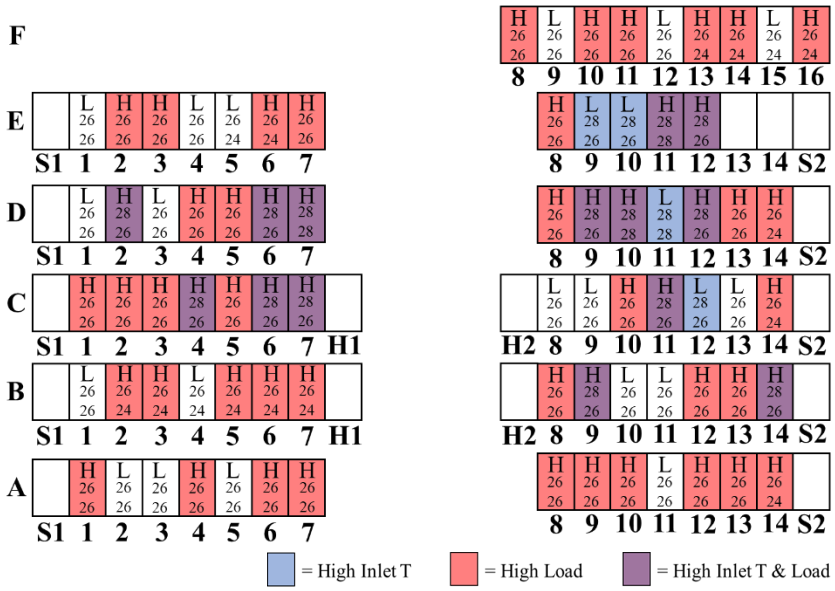

Figure 31. Scenario B – High inlet temperature and load (bird's-eye view)

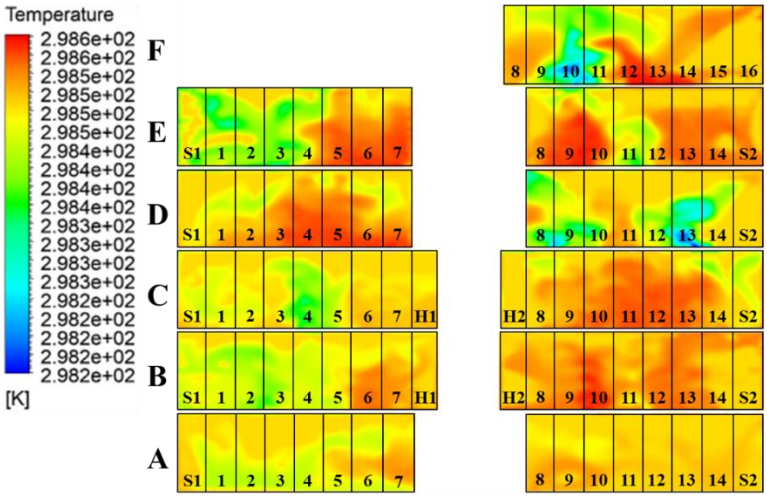

Figure 32. Scenario B – Front of rack temperature distribution

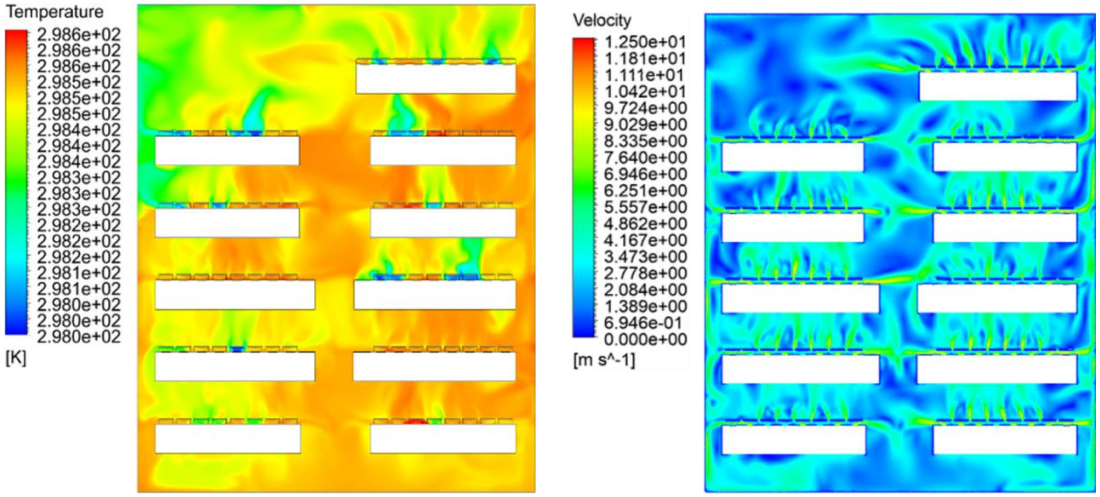

Figure 33 & 34. Scenario B – Temperature and velocity distribution, 1m XY plane

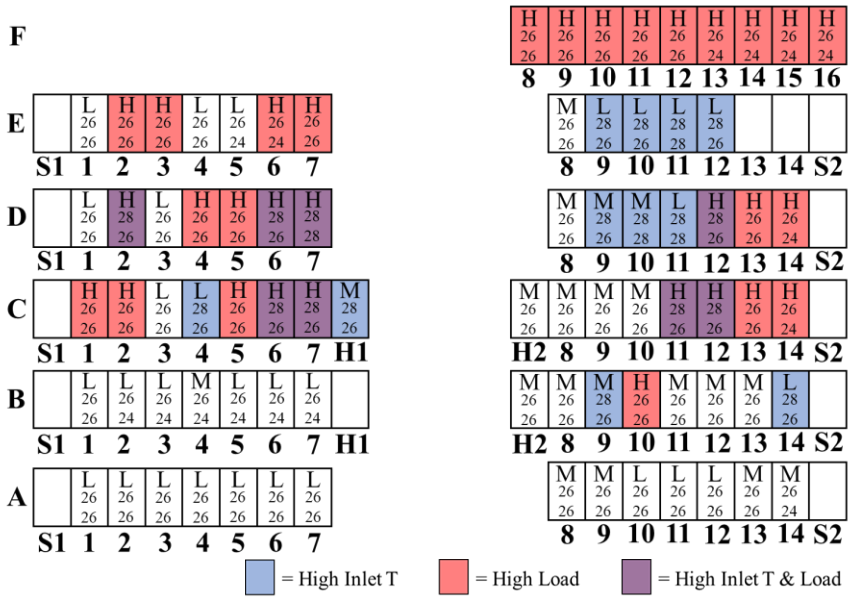

Figure 35. Scenario C – High inlet temperature and load (bird's-eye view)

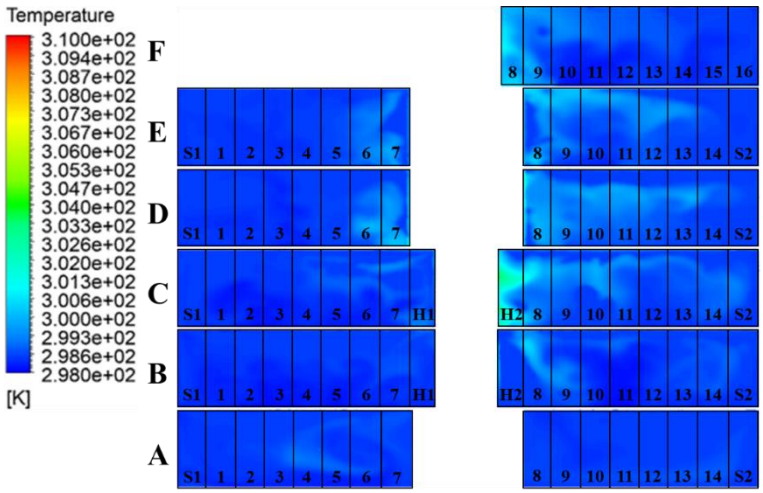

Figure 36. Scenario C – Front of rack temperature distribution

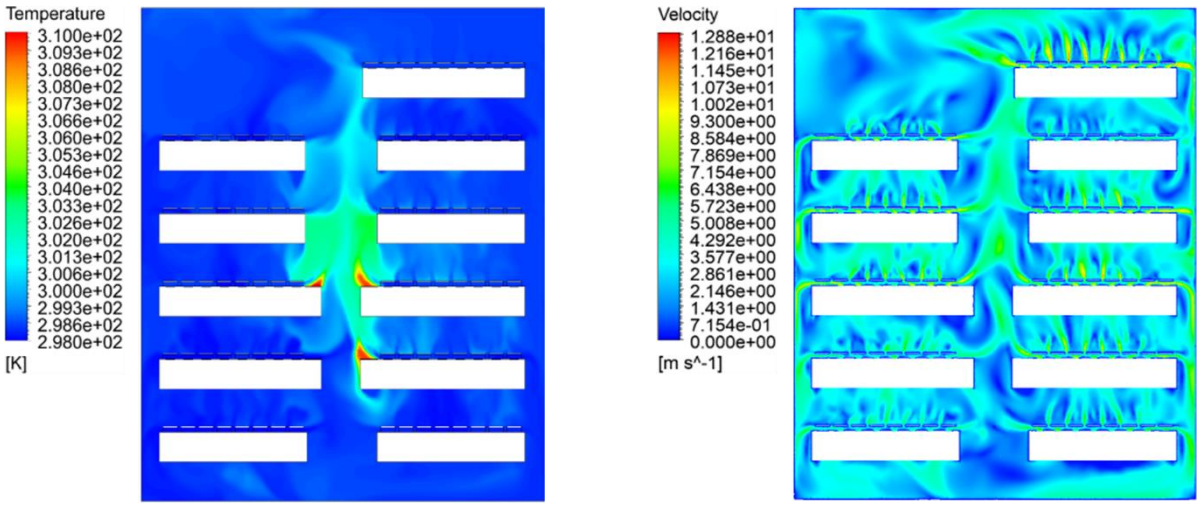

Figure 37 & 38. Scenario C – Temperature and velocity distribution, 1m XY plane

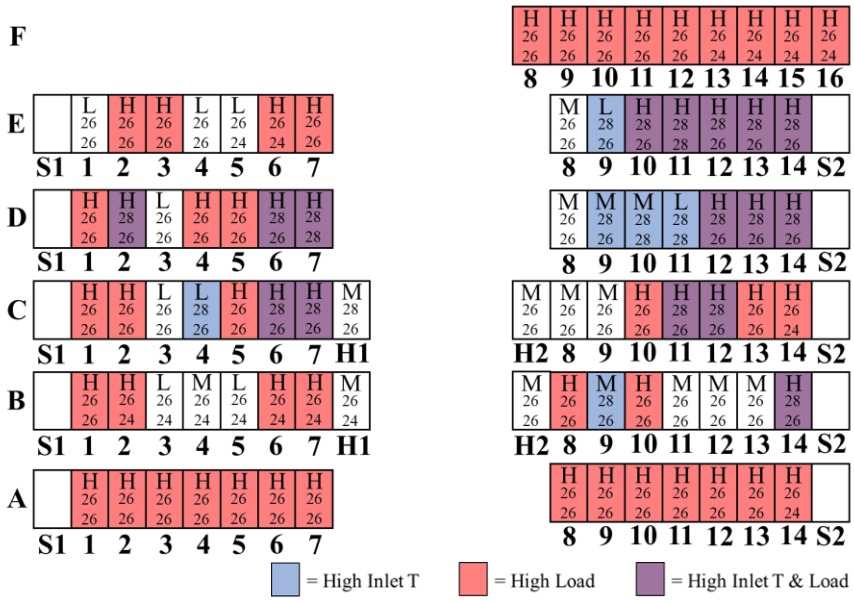

Figure 39. Scenario D – High inlet temperature and load (bird's-eye view)

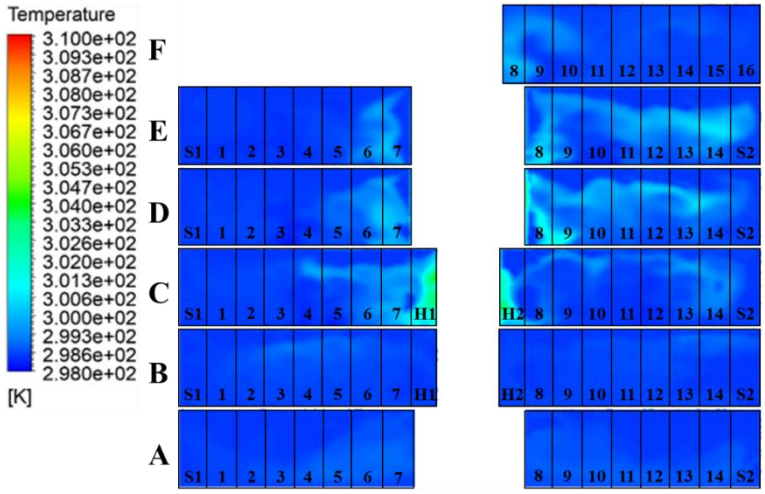

Figure 40. Scenario D – Front of rack temperature distribution

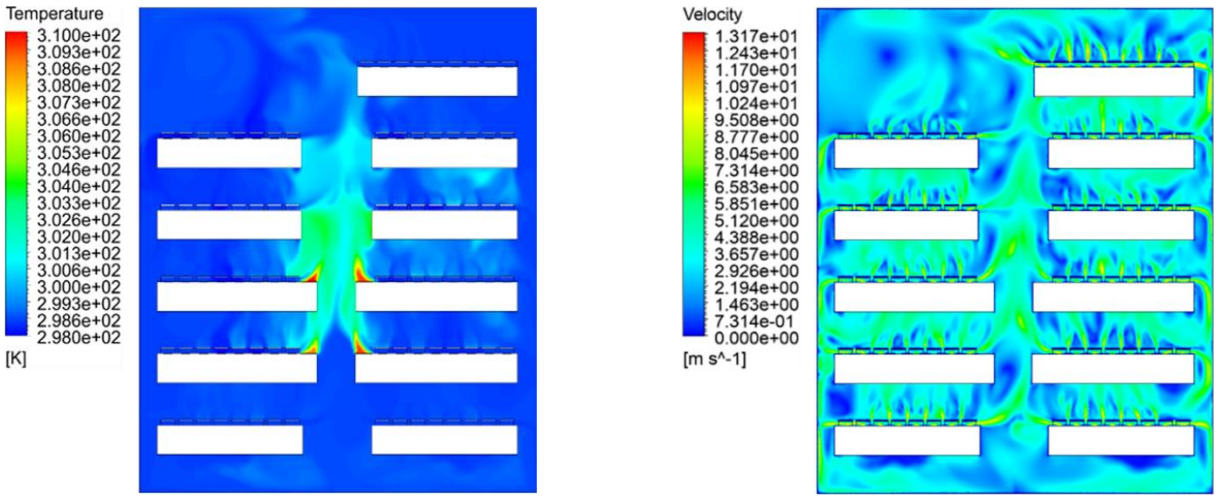

Figure 41 & 42. Scenario D – Temperature and velocity distribution, 1m XY plane

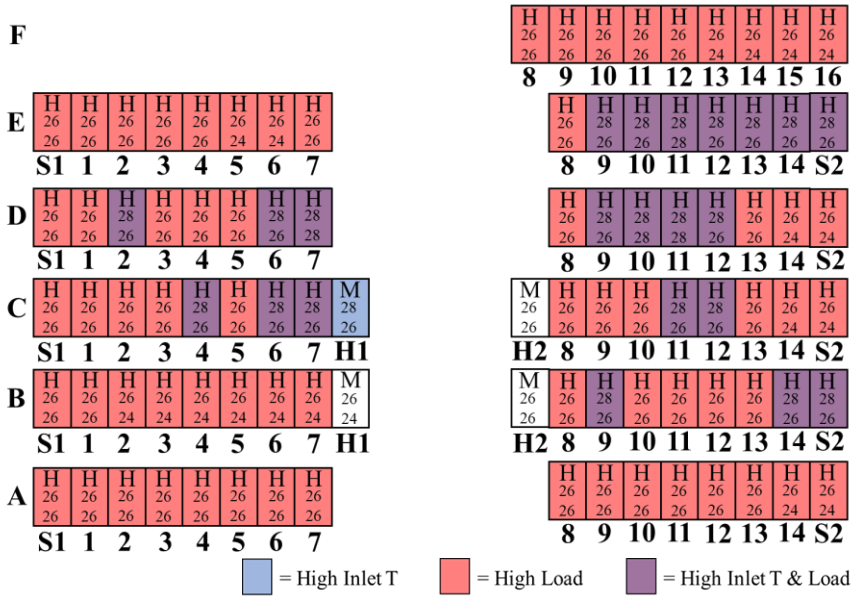

Figure 43. Scenario E – High inlet temperature and load (bird's-eye view)

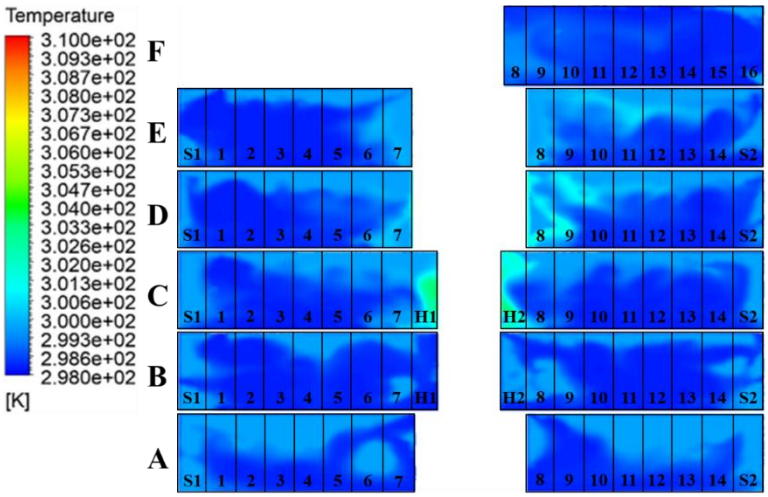

Figure 44. Scenario E – Front of rack temperature distribution

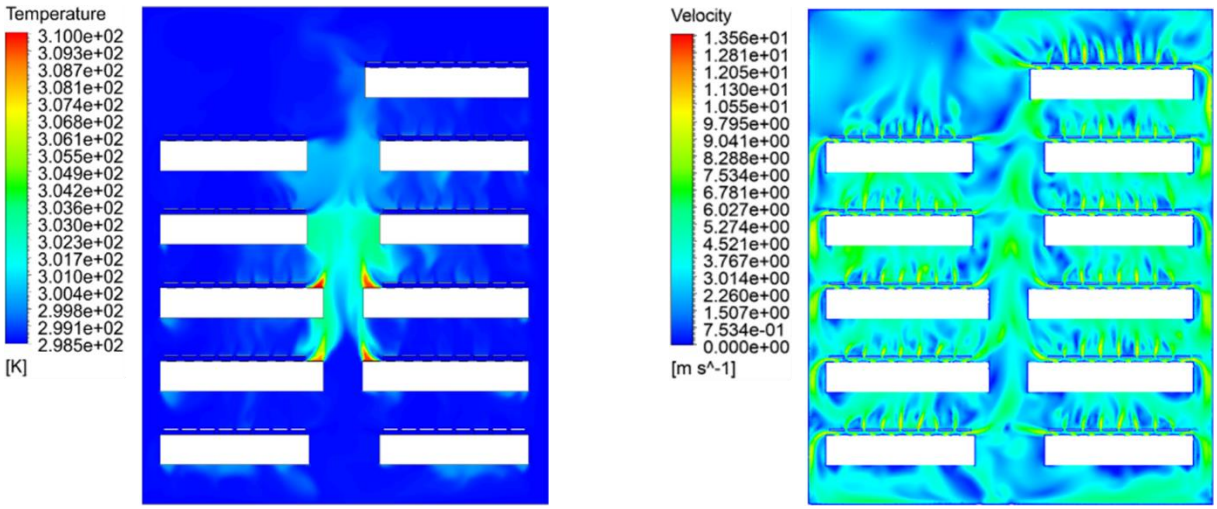

Figure 45 & 46. Scenario E – Temperature and velocity distribution, 1m XY plane

4. Discussion

4.1 Server model

Computer servers, like the Dell Poweredge 1750 used in this report, are designed to maximise the dissipation of heat produced in the server. Forced convection is a method used in computer servers to increase the rate of heat transfer. The fans present in the Dell Poweredge 1750 are situated adjacent to the PSU and the CPUs, in order to increase the rate of heat transfer at these components.

Fig 7-18 show the temperature distribution at plane 3 for loading conditions with inlet temperature ranging from 24-28°C. The corresponding velocity profile for each loading condition with the same inlet temperature is shown in Fig 19-30. Idle loading conditions considered heatsink surface temperatures with the same relation, (inlet temperature +1°C) to simulate the server in an idle state. The assumption was made that at an idle state the components in a server were operating at 1°C above ambient temperature.

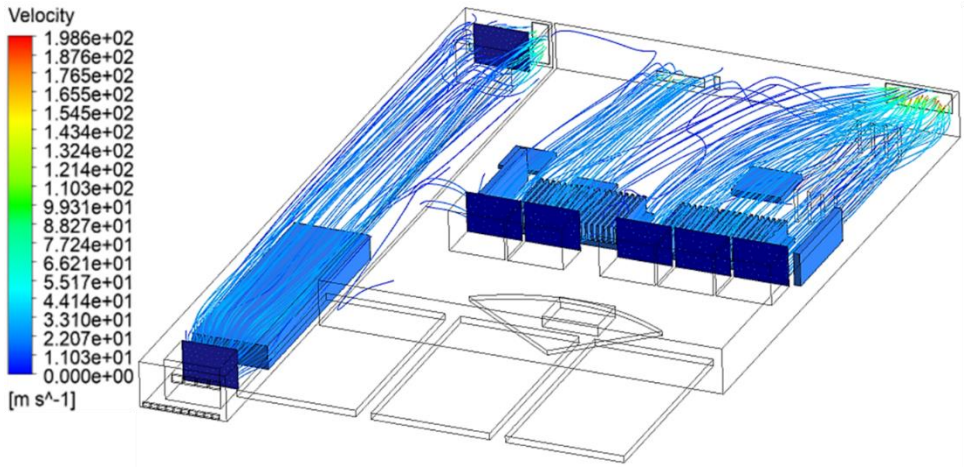

Figure 47. Velocity pathway from server fans (Inlet T = 26°C, Load = V.High)

The CPU is the main processing unit in the server and therefore generates the most heat. As the server load increases the temperature of the components in the model increase as presented in Table 3. For all of the inlet temperatures tested with medium, high, and very high loading condition, the highest temperature region occurs at the same point. Fig 13 shows the temperature distribution for a high loading condition with inlet temperature at 26°C. The corresponding velocity profile for this loading condition is shown in Fig 25. Looking at the temperature distribution and velocity profile together, as expected, a high temperature region occurs where there is low velocity, and a low temperature region occurs where there is high velocity. Looking closely at Fig 47, there is an area of the CPU heatsink situated on the left of the server which doesn't receive the same level of forced convection due to a break in the arrangement of the fans. As a result, the highest temperature region occurs at this point for all loading condition tested excluding the idle case.

4.2 Data hall model

Scenario B contains an inlet temperature range between 24-28°C. High inlet temperature areas and loads for scenario B are indicated in Fig 31. Scenario B contains concentrated higher loaded racks scattered over the data hall. The front of rack temperature distribution displayed in Fig

32, shows where higher temperature affects the front of rack temperature. For example, in scenario B higher loaded racks numbered C1-C7 result in a higher front of rack temperature region at racks numbered D2-D7 shown in Fig 32. Similarly, low loaded racks numbered B9 and B10 in Fig 31 have resulted in a lower front of rack temperature region at racks numbered C9-C11. This can be explained by looking at the temperature distribution and velocity profile displayed in Fig 33 and 34. The higher back of rack temperatures produced from heavily loaded racks affect the temperature distribution at the front of the rack's opposite. Scenario B contains spare racks at the end of each row and an extra two spare racks located at E13 and E14 as shown in Fig 31. The temperature distribution at 1m shown in Fig 33, shows a higher temperature region near racks E11-E14. Looking at the velocity distribution in Fig 34, a low velocity region occurs at the back of rack's E11-E14. Due to the unoperated racks at E13 and E14 there is poor airflow which as a result, elevates the temperature around that area. It is noticed that the temperature difference in data hall scenario B is very small. Employing rear door heat exchangers is an extremely efficient method used in cooling data centres. From experimental data collected using the ColdLogik user interface, when rack C3 was operating with a middle of the rack temperature of 44.9°C for example, the back of rack temperature was 25.7°C. Even when racks are running at high power densities the hybrid cooling system in place can still maintain an average ambient temperature between 25-26°C.

As mentioned previously, scenario C was created to represent the data hall condition at the time of experimental data collection. Scenario C, D and E contain racks operating at similar inlet temperature but with increasing load. Scenario C contains the same spare unoperated racks as scenario B with three additional uncooled racks operating in the centre of the data hall. The uncooled racks have no cooling architecture and therefore pump hot, untreated air from the servers in the rack directly into the room. Scenario D and E also contain uncooled racks in the centre; however, scenario D contains an extra uncooled rack as shown in Fig 39. Scenario D also contains operated spare racks, E13 and E14 with all other spare racks remaining unoperated. Scenario E contains the maximum loading scenario in the data hall. It contains the same uncooled racks as scenario D with all available racks including spare racks operating at full load.

The temperature distribution in scenario C, Fig 37, shows the uncooled racks BH2, CH1 and CH2 produce a higher temperature region around the centre of the hall. This is helped by the velocity produced from the adjacent cooled racks. The velocity from the adjacent cooled racks acts as a barrier which creates a channel down the centre of the hall for the hot uncooled air to flow, as shown in the velocity distribution in Fig 38. This has a detrimental effect on the front of rack temperature distribution. As a result of the uncooled racks, front of rack temperatures of around 30°C occur at rack CH2 and around 28°C at other areas seen in Fig 36. Due to the unobstructed airflow through the centre of the data hall the untreated air travels as far as row F. Scenario D contains an increase in heavily loaded rack positions as shown in Fig 39. As mentioned previously scenario D also contains an extra uncooled rack in the centre of the hall. Looking at the front of rack temperature distribution for scenario D shown in Fig 40, the addition of an extra uncooled rack produces high temperature regions at the front of rack's CH2 and CH1. Due to the increase in heavily loaded racks, there is a higher velocity region through the centre of the hall as shown in Fig 42. Racks C8-C9, D8-D11 and E8-E9, positioned adjacent to the centre of the hall, contain low and medium loaded racks. These racks produce a lower velocity region at the back of the rack which allows the untreated air to travel further in between rows. This is because the high velocity region in the centre of the hall is allowed to push the air down the row further away from the centre, this results in a greater front of rack temperature distribution at racks E8-ES2 and D8-DS2. At the opposite side of the hall, racks C5-C7, D4-D7

and E6-E7 contain heavily loaded racks which have a higher velocity region at the back of the rack. This higher velocity region acts as barrier which resists the flow of air down the row. This results in a lower front of rack temperature distribution at the left-hand side of the hall for row C, D and E.

As shown in Fig 43, scenario E has been created to simulate maximum load in the data hall. All available cooled racks contain high loads and there are four uncooled racks operating in the centre of the hall. Due to racks operating at higher load there are higher velocity regions between rows as shown in Fig 46. The combination of high velocity distribution and untreated air from the uncooled racks results in a much greater front of rack temperature distribution. The tops of the front of the racks in each row are subject to a higher temperature distribution as shown in Fig 44. Racks CH1, CH2, and D8-D10 show where the highest front of rack temperature occurs, at around 31°C.

5. Conclusion

This paper presents the modelling of a data centre at server, rack, and room level with the use of field measurements performed. From the server simulations carried out it was found that the dissipation of heat was directly related to the velocity profile in the server. This is expected as the fans in the server are located to maximise the rate of convection at the heatsinks on the processing units. A break in the arrangement of the server fans highlighted an area on one of the heatsinks which may receive insufficient cooling. It is worth noting that the heat sources in the server model were modelled with a constant surface temperature. This meant that all areas of the heatsinks on the processing units were operating at the same temperature when in reality the outer extremities may operate at a lower temperature to the centre. From analysing the front of rack temperature distribution for scenarios B-E it was found that elevated temperatures were generated at the front of racks that opposed the rear of the higher loaded racks. This is expected as the higher loaded racks exhaust higher back of rack temperatures onto the front of the racks opposite. It was also found that clusters of three or more higher loaded racks situated together have a greater influence on the opposing front of rack temperatures. When a higher loaded rack is isolated the exhausted back of rack temperature is susceptible to a greater rate of diffusion and therefore has less of an effect on the opposing front of rack temperature. For scenarios with operated uncooled racks, resulting front of rack temperature distribution is heavily influenced by the velocity produced from adjacent racks. The velocity produced from low, medium and high loaded racks, has a varying effect on the back of rack temperature and velocity of the uncooled racks. If higher loaded racks, which accommodate higher velocity, are positioned strategically in the hall the detrimental effect of the hot uncooled racks can be abated. If all available racks are operating at a maximum level, large areas of the data hall are susceptible to temperatures of up to 31°C. If the data hall is operating at full load with the presence of uncooled racks, thermal management complications may arise which could lead to overheating of components or even system failure.

References

[1] Kant, K., "Data Centre Evolution: A tutorial on the state of the art, issues and challenges", Computer Networks 53 (2009) : 2939-2965.

[2] Dumsky, D., Isaev, E., "Data centres for physical research", Physics Procedia 71 (2015) : 298-302.

[3] Daim, T., Bhatla, A., Mansour, M., "Site selection for a data centre – a multi-criteria decision-making model", International Journal of Sustainable Engineering 6 (1) (2012) : 10-12.
[4] Kamiya, G., "Data centres and data transmission networks", https://www.iea.org/tcep/ buildings/datacentres/ (2019).
[5] Oro, E., Depoorter, V., Garcia, A., Salom, J., "Energy efficiency and renewable energy integration in data centres. strategies and modelling review", Renewable and Sustainable Energy Reviews 42 (C) (2015) : 429-445.
[6] Rasmussen, N., "The different types of air distribution for IT environments", Schneider Electric (2017).
[7] Chi, YQ., Summer, J., Hopton, P., "Case study of a data centre using enclosed, immersed, direct liquid-cooled servers", Annual IEEE Semiconductor Thermal Measurement and Management (2014) : 164-173.
[8] Jinkyun, C., Byungseon, S., "Evaluation of air management system's thermal performance for superior cooling efficiency in high-density data centres", Energy and Buildings 43 (9) (2011) : 2145-2155.
[9] Almoli, A., Thompson, A., Kapur, N., Summers, J., Thompson, H., Hannah, G., "Computational fluid dynamic investigation of liquid rack cooling in data centres", Applied Energy 89 (1) (2012) : 150-155.
[10] Choi, J., Youngjae, K., Sivasubramaniam, A., Srebric, J., "A CFD-Based tool for studying temperature in Rack-Mounted servers", IEEE Transactions on Computers 57 (8) (2008) : 1129-1142.
[11] Fakhim, B., Behnia, M., Armfield, S.W., Srinarayana, N., Fakhim, B et al., "Cooling solutions in an operational data centre: a case study", Applied Thermal Energy 31 (14-15) (2011) : 2279-2291.
[12] Wibron, E., "A numerical and experimental study of airflow in data centres", Lulea University of Technology (2018).
[13] Leschziner, M. "Statistical turbulence modelling for fluid dynamics", Imperial College Press (2015).
[14] Milnes, J., Drikakis, D., "Qualitive assessment of RANS models for hypervapotron flow and heat transfer", Fusion Engineering and Design 84 (7-11) (2009) : 1305-1312.
[15] Smirnov, P., Menter, F., "Sensitization of the SST turbulence model to rotation and curvature by applying the Spalart-Shur correction term", Journal of Turbomachinery 131 (4) (2009) : 297-302.